FernUniversität in Hagen
Faculty of Mathematics and Computer Science

Artificial Intelligence Group

Investigating global steel cycle modelling techniques and simulating climate mitigation and adaptation scenarios

Bachelor's Thesis

in partial fulfillment of the requirements for
the degree of Bachelor of Science (B.Sc.)
in Computer Science

submitted by
Merlin Jo Hosak

First examiner:	Dr. Jandson Santos Ribeiro Santos Artificial Intelligence Group
Advisor:	Dr. Jakob Dürrwächter Potsdam Institute for Climate Impact Research (PIK)

Statement

Ich erkläre, dass ich die Bachelorarbeit selbstständig und ohne unzulässige Inanspruchnahme Dritter verfasst habe. Ich habe dabei nur die angegebenen Quellen und Hilfsmittel verwendet und die aus diesen wörtlich oder sinngemäß entnommenen Stellen als solche kenntlich gemacht. Die Versicherung selbstständiger Arbeit gilt auch für enthaltene Zeichnungen, Skizzen oder graphische Darstellungen. Die Bachelorarbeit wurde bisher in gleicher oder ähnlicher Form weder derselben noch einer anderen Prüfungsbehörde vorgelegt und auch nicht veröffentlicht. Mit der Abgabe der elektronischen Fassung der endgültigen Version der Bachelorarbeit nehme ich zur Kenntnis, dass diese mit Hilfe eines Plagiatserkennungsdienstes auf enthaltene Plagiate geprüft werden kann und ausschließlich für Prüfungszwecke gespeichert wird.

	Yes	No
I agree to have this thesis published in the library.	☑	☐
I agree to have this thesis published on the webpage of the artificial intelligence group.	☑	☐
The thesis text is available under a Creative Commons License (CC BY-SA 4.0).	☐	☑
The source code is available under a GNU General Public License (GPLv3).	☐	☑
The collected data is available under a Creative Commons License (CC BY-SA 4.0).	☐	☑

Leeds, 21st of February 2024 M. Hosak

(Place, Date) (Signature)

Abstract

Global steel and iron production is responsible for 7.2 % of global greenhouse gases [Rit20]. To find emission-reduction strategies in this sector, researchers build global models of the steel cycle using a variety of modelling approaches and prediction techniques.

This thesis investigates *inflow-driven* and *stock-driven* dynamic stock modelling and proposes a new *change-driven* modelling approach. Additionally, the prediction technique by *Pauliuk* et al. [PWMA13] is compared to an approach proposed by Prof. *Dürrwächter* as well as a new machine learning-based technique using long short-term memory (*LSTM*) networks.

The three model approaches and three prediction techniques are implemented and combined to produce nine forecasts of the global steel production. Here, data available in 2008 is used to predict the years 2009-2022. Subsequently, this is compared to the actual production data in this time period to assess the performance of the methods.

Strengths and weaknesses of the six used methods are discussed. Overall, *inflow-driven* models and *LSTM* predictions performed best. The most accurate predicting model combination was the *change-driven* approach combined with the *LSTM* producing predictions with a mean absolute percentage error of 4.45 %. However, due to implausible lifetime projections in the *change-driven* model, its use was discouraged.

Hence, the *inflow-driven* approach combined with the *LSTM* prediction is used to derive final predictions. The resulting global production forecast suggest that the global steel demand until 2100 might be 25 % higher than previously [PWMA13] assumed, resulting in higher greenhouse gas emissions.

Contents

1. Introduction **1**
- 1.1. Related Work . . . 2
- 1.2. Goal . . . 2
- 1.3. Overview . . . 3

2. Preliminaries **3**
- 2.1. Dynamic stock modelling . . . 3
- 2.2. (Dynamic) Material Flow Analysis . . . 4
- 2.3. Steel stock prediction . . . 5
- 2.4. Long short-term memory networks . . . 6
- 2.5. Steel cycle modelling . . . 7

3. Methods **8**
- 3.1. Experiment structure . . . 9
- 3.2. Data sources & preparation . . . 9
- 3.3. SIMSON upper cycle . . . 12
- 3.4. Model approaches . . . 13
  - 3.4.1. Inflow-driven model . . . 14
  - 3.4.2. Stock-driven model . . . 16
  - 3.4.3. Change-driven model . . . 17
- 3.5. Prediction techniques . . . 19
  - 3.5.1. Pauliuk prediction . . . 20
  - 3.5.2. Dürrwächter prediction . . . 22
  - 3.5.3. LSTM prediction . . . 23
- 3.6. Evaluation . . . 25

4. Results **25**
- 4.1. Pre-Evaluation of LSTM Models . . . 26
- 4.2. Predictions . . . 26
- 4.3. Runtime . . . 27

5. Discussion **28**
- 5.1. Model approaches . . . 29
- 5.2. Prediction techniques . . . 30
- 5.3. Analysis of predictions . . . 31
- 5.4. SSP scenario predictions . . . 34

6. Conclusion **36**

References **38**

A. Specifics of SIMSON **42**
- A.1. Flows . . . 42

A.2. Calculation of EAF/BOF Route 43
A.3. Other functionalities 44
A.4. Code 45

B. Mapping of regions **45**

1. Introduction

Energy usage in industry is responsible for nearly a quarter of global greenhouse gas emissions. Iron and steel production accounts for the biggest proportion of that, 7.2 % in total [Rit20] (s. Fig. 1). Following the 2015 Paris agreement, governments worldwide set targets to decarbonise their industries and ultimately also their iron and steel production.

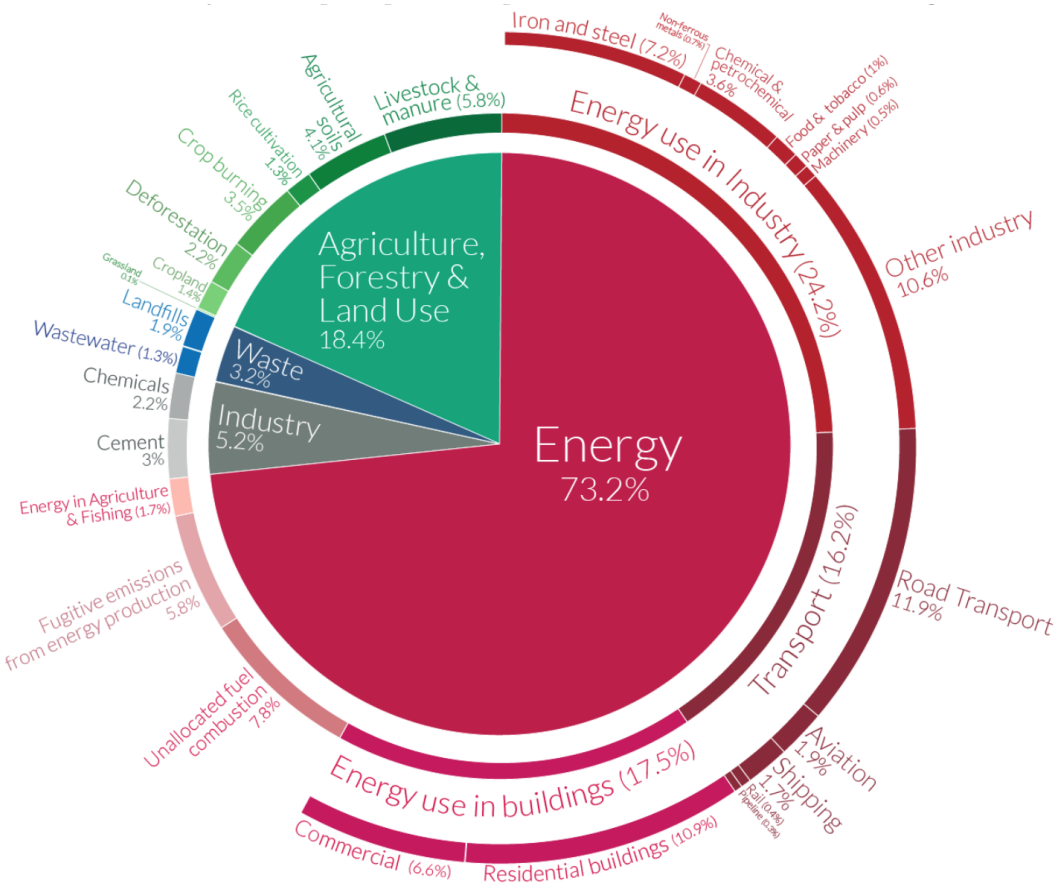

Figure 1: Iron and Steel production share in global greenhouse gas emissions (Figure taken from [Rit20]).

There are a variety of methods to achieve these targets in this sector. These include subsidising steel recycling, producing materials more efficiently, replacing steel with more sustainable materials like wood or investing in technologies to reuse steel directly instead of remelting it during recycling. However, it is not always clear which of these methods is the most successful in decarbonisation, especially in relation to their costs.

To explore these - and many more - challenges, the Potsdam Institute for Cli-

mate Impact Research (PIK) requires a model of the global steel cycle, as part of their model of the Earth's energy-economy-emissions system, REMIND ([BBB+21], s. Section 2.5).

Modelling and predicting the steel cycle is complicated - an adequate representation in stocks and flows needs to be developed and available data needs to be found, analysed and realistically incorporated. Prof. Stefan Pauliuk first approached this feat in depth in his much cited 2013 work [PWM13][PWMA13]. But his approach and predictions are ten years old and several new methods have since been developed. Additionally, with the rise of artificial intelligence over the last years, the question presents itself whether and how machine learning techniques could be applied in this field.

1.1. Related Work

A lot of the background for this project is in these 2013 papers from Prof. Stefan Pauliuk and Prof. Daniel B. Müller: 'Steel all over the world: Estimating in-use stocks of iron for 200 countries', 'The steel scrap age' and 'Carbon emissions of infrastructure development'. They provided a first estimate of global 'in-use' steel stocks, the total amount of steel currently present in construction, cars, products, etc. in each country of the world [PWM13]. Based on this, they predicted the development of these stocks and analysed the effect on steel production and steel scrap generation in the coming decades.

Some major findings of their work suggest that if steel demand trends continue, the energy demand of the steel sector will be immense, threatening the target to limit the global temperature increase to below 2°C [MLL+13] as well as building up large stocks of steel scrap that cannot be recycled [PWMA13]. These examples showcase the efficacy of such models to predict potential risks and unforeseen dynamics.

Several other models of the steel cycle have since proposed [RTLW+22, IEA22, YWM21]. They all use techniques such as Material Flow Analysis (MFA) and Dynamic Stock Modelling (DSM) to set up their models. Predictions are often based on analysing past stock behaviour and coming up with a formula to predict steel stocks, estimating the rest of the model from there.

1.2. Goal

This thesis will analyse Pauliuk and others' approaches to steel cycle modelling and prediction, and develop a method to test and compare them. This will then be used to propose an updated model (SIMSON, s. Section 2.5), to serve as a basis for steel economy modelling in REMIND. Three modelling and three prediction approaches will be examined and combined to assess how well they would have predicted the last 14 years (2009-2022) of the global steel cycle.

1.3. Overview

Tools and techniques that are needed throughout the thesis are discussed in Section 2. In Section 3, the setup and methodology of the experiments is discussed in detail.

Subsequently, the results are presented in Section 4, followed by a discussion of them in Section 5. Lastly, the thesis is concluded in Section 6, including an outlook on possible future work in this field.

2. Preliminaries

Before explaining the concrete setup and design of the investigation, this section explains some of the tools used in more detail. Sections 2.1 and 2.2 cover dynamic stock modelling and material flow analysis as the basis of global steel modelling. In section 2.3, previous research and techniques on steel stock prediction are summarised. Long short-term memory networks as a potential new machine-learning based approach to steel stock prediction is presented in section 2.4. Lastly, in section 2.5 an overview of SIMSON, the model which this investigation aims to inform, is given.

2.1. Dynamic stock modelling

Dynamic stock modelling (DSM) is a method to relate inflows, outflows, stocks and lifetimes of a material in a process to each other. In our case, this is steel in the use-phase, so the steel currently in use in various products in the world (measured in weight (here: metric tonnes)). A visualisation is depicted in Fig. 2.

The inflow is the steel in new products, such as new cars or buildings. The stock is the total amount of steel that is in use in a given time period. At some point, the steel leaves the use phase again because it reaches its 'end-of-life' and then gets recycled or ends up in landfills. This point is defined by the steel's lifetime - cars might for example have an average lifetime of 30 years. Lastly, the amount of steel reaching its end of life in a given time period represents the outflow of the model.

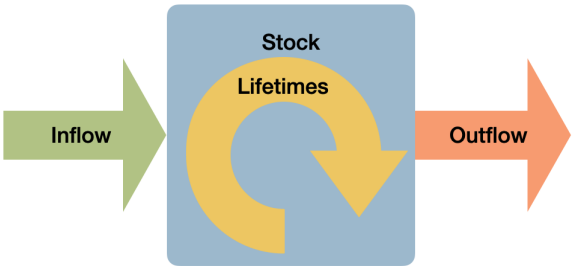

Figure 2: Overview of dynamic stock modelling.

In DSM it is assumed that a product might have a lifetime mean τ, with standard

deviation (SD) σ so that the steel inflow into the stock in a given year leaves the stock (outflow) according to the normal (Gaussian) probability distribution function (here λ). Hence the following Eqs. 1-4 can be used to relate the entities to one another [PWMA13].

$$S_c(t) = I(t) - O(t) \tag{1}$$

$$S(t) = \sum_{t' \leq t} S_c(t') \tag{2}$$

$$\lambda(t, t', \tau, \sigma) = \frac{1}{\sqrt{2}\pi\sigma} e^{\frac{-(t-t'-\tau)^2}{2\sigma^2}} \tag{3}$$

$$O(t) = \sum_{t' \leq t} I(t')\lambda(t, t', \tau, \sigma) \tag{4}$$

Here, $I(t)$ denotes the inflow in a given year t, $O(t)$ the outflow, $S(t)$ the stocks and $S_c(t)$ the stock change.

There are two popular approaches in dynamic stock modelling: the *inflow-driven* and the *stock-driven* approach. In the former, inflow data and lifetime estimates are used to obtain stocks and outflow, whereas with the latter, stock and lifetime data are used to estimate inflow and outflow.

Note that technically, given any two of the four quantities inflows, stocks, outflows and lifetimes Eqs. 1-4 can be used to estimate the other two (given that lifetime mean and SD might change over time).

2.2. (Dynamic) Material Flow Analysis

Material flow analysis (MFA) is a technique to quantify the life cycle of materials and substances. Its structure is made out of processes, flows between those processes and stocks within a process. In the steel cycle, there might for example be a process 'Use-phase', a flow from production to the use phase and stocks of steel accumulating in the use-phase, for example in buildings. A visualisation of the structure of a simple MFA from Pauliuk (2011) is shown in Fig. 3.

Two more aspects define MFAs. Firstly, MFAs always have a spatial and a temporal boundary. Processes, flows and stocks are examined within a clearly defined region over a specific period of time as well as flows into and out of this region. Secondly, mass balance always must always be ensured in an MFA. This means that the sum of inflows minus the sum of outflows of a process must always equal the change of stocks in a process. If there are no stocks being accumulated in a process, e.g. in the 'Production' process in Fig. 3, this stock change must be zero.

Dynamic Material Flow Analysis (DMFA) is a sub-discipline of MFA. Here, several MFAs are developed over a longer period of time. Rostek et al. for example conducted an investigation into how the steel cycle in the EU changed between 2002 and 2019 [RTLW$^+$22]. Hence, they created an MFA for each year in the time frame and could analyse the change of stocks and flows in the cycle over 18 years.

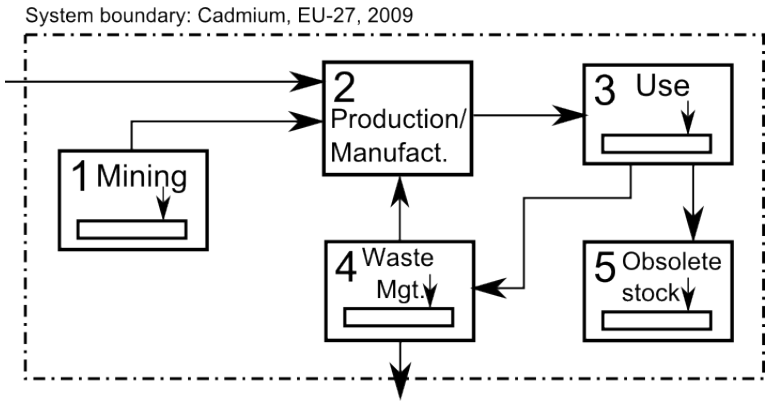

Figure 3: A simple MFA example of the flow of Cadmium with the EU (space) and the year 2009 (time) as the system boundaries, taken from [Pau11]. Five processes are displayed and numbered.

2.3. Steel stock prediction

Dynamic stock modelling and material flow analysis provide the required tools to approach steel cycle modelling. Concerning the past, data on flows, stocks and lifetimes can be gathered to inform the model. This section describes how predicting the future of such models has been addressed in other work.

A particular area of interest in this field is how global steel production will change due to its greenhouse gas emissions. One approach could be to establish trends based on past production.

However, the approach taken more commonly is to predict steel stock development first and then infer production from there (s. [PWMA13, YWM21, PSL23]). This is based on the assumption that "service level is coupled to stock level" [PWMA13], so that the per-capita steel stocks represent how much a society uses the *services* steel helps to provide (housing, transport, etc., s. also [PFH$^+$21]).

The development of stock predictions is helped by two factors: unlike production, stocks are independent of trade patterns, and stock levels are strongly correlated to economic development. This can be observed in Fig. 4 - the correlation coefficient of the two dataset used in the figure [MLL$^+$13, JGMG12] is roughly 0.87, indicating a high and positive correlation.

Hence, steel stocks can be predicted by defining some kind of relationship between steel stocks and economic development from past data and then using predictions of economic development to obtain future stocks. There have been several of such investigations [PWMA13, YWM21, PSL23], and they mostly differ in how economic development is matched to stocks and what predictions of economic development are used.

For example, Pauliuk et al. point out that in industrialised countries, it appears that per capita steel stocks are starting to saturate (see eg. USA data in Fig. 4)

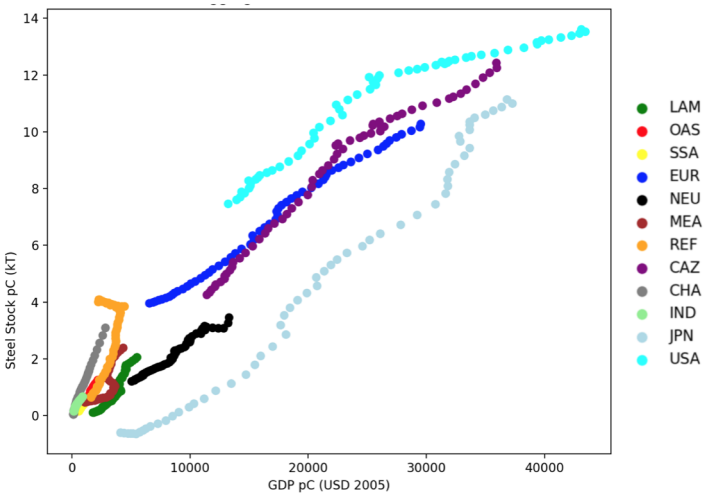

Figure 4: Steel stock per capita development over gross domestic product (GDP) per capita in twelve world regions (s. [BBB+21]), 1950-2008. Stock data from [MLL+13], GDP data from [JGMG12].

and hence proposes that steel stocks saturate over time, at a level of economic development roughly similar to that of industrialised nations currently [PWMA13]. This idea has been adopted by various researchers [PSL23] [YWM21] and has been featured in the United Nations intergovernmental panel on climate change (IPCC) reports [BNA+22].

2.4. Long short-term memory networks

Long short-term memory (LSTM) networks, are a type of recurrent neural networks (RNN) proposed by Hochreiter and Schmidhuber [HS97]. They have been shown to be especially useful for time series prediction [SNTSN18]. LSTM networks consist of custom LSTM cells, similar to RNN cells with the added functionality of three gates that are optimised to determine how much of the last cell state to remember (forget gate), how much of the new information should be incorporated (input gate) and how much information shall be passed to the next LSTM cell (output gate), s. Fig. 5.

The key feature of LSTM cells is the cell state - the horizontal line running through the top of Fig. 5 and is continually updated. It has the ability to capture long-term dependencies ('remember' patterns from the past), in contrast to traditional RNNs, where information from long ago tends to get lost (vanishing/exploding gradient problem, [BSK19]). Hence they are particularly suited for time series forecasting, as observed patterns might have already occurred in the past, giving the network some information on what is likely to happen next.

The effectiveness of LSTM-networks for time series forecasting has been shown

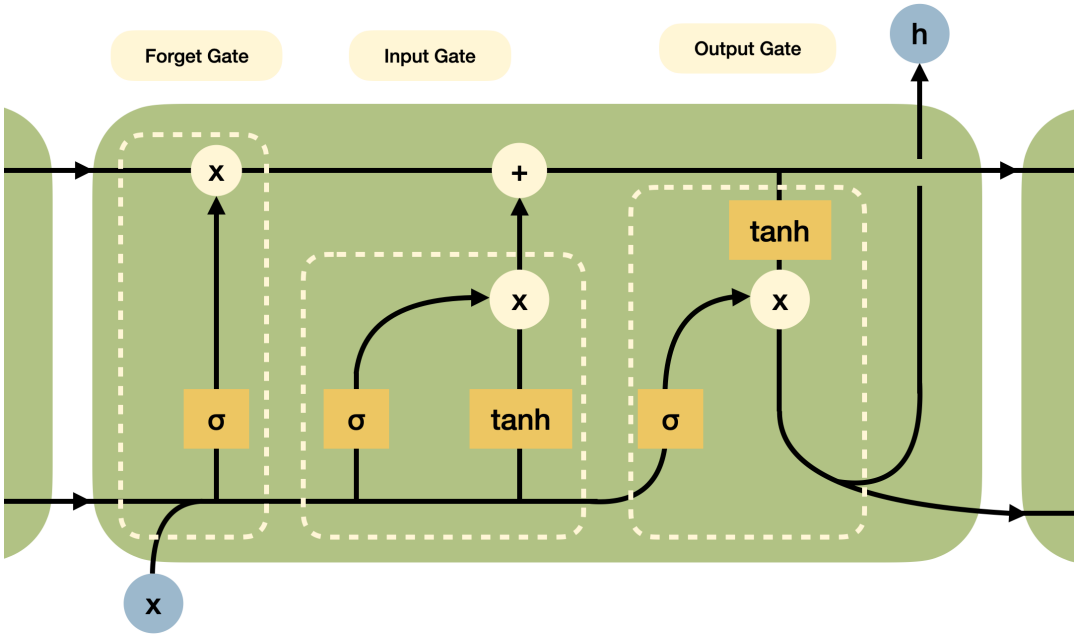

Figure 5: Structure of a LSTM cell within a LSTM network with input x and output h, based on [Mun21]. The gates are implemented using sigmoid- (σ) and $tanh$ activation functions as well as point wise addition $+$ and multiplication x operators [SK18].

in related fields like oil production [SK18] and weather forecasting [KS20].

2.5. Steel cycle modelling

The Potsdam Institute for Climate Impact Research (PIK) is modelling the global economy-energy-emissions system in their integrated assessment model (IAM), REMIND (Regional Model of INvestments and Development) [BBB+21]. IAMs consist of sub-modules representing various aspects of the system. In REMIND's case, this includes models on global investments, energy-system costs and carbon-intensive industries [BBB+21].

Concerning steel, the PIK is aiming to build on past research [PSL23] to create an MFA-based model of the global steel cycle, that can interact with the economy-based modules in REMIND to project a realistic development and, ultimately, the carbon emissions of the industry.

As a potential solution, this investigation presents the model SIMSON (Simulating In-Use Material Stocks with the ODYM Network). SIMSON covers steel production along two routes, via basic oxygen- (BOF) or electric arc furnace (EAF), uses the four in-use categories ([PWMA13]) and eight steel-scrap categories (based on [RTLW+22], [Wit21]). It covers the global steel production across the twelve REMIND world regions [BBB+21]. The model is implemented in Python and uses the

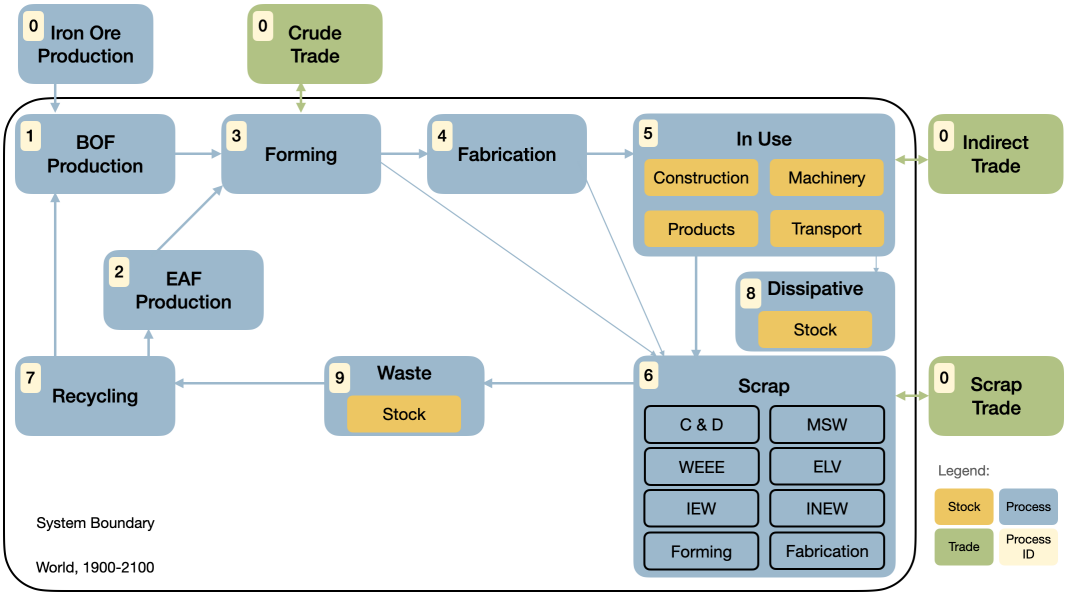

Figure 6: Structure of SIMSON.

ODYM library [PH19].

Whilst the structure of SIMSON (Fig. 6) was developed in collaboration with Dr. Jakob Dürrwächter (PIK), this investigation contributes the development data input of the 'upper part' of the cycle (production - use phase) including the prediction of the steel stocks, which serves as the basis of the rest of the model.

After methodically describing this model preparation and prediction process, a first application of the resulting predictions in SIMSON, including individual predictions for the shared socio-economic path scenarios (SSP, [OKR+14]), forecasting global steel production until 2100 is presented in Section 5.4. There are five SSP scenarios that denote a range from more sustainable development (SSP1) to scenarios where society does not limit its greenhouse gas emissions (SSP5). Climate impact researchers often use these scenarios to make it easier to compare their research [PSL23].

3. Methods

After summarising the techniques and models relevant for this thesis, this chapter discusses the experiments in detail. Firstly, the setup of the experiments and the idea behind the thesis' structure is presented in Section 3.1. In Section 3.2 the choice of data used is discussed alongside its preparation. Subsequently, the functionality of SIMSON that this thesis aims to inform is described in detail in Section 3.3.

In Section 3.4 the implementation of the model approaches is described followed by the prediction techniques in Section 3.5. Lastly, the evaluation of the resulting

predictions is discussed in Section 3.6.

3.1. Experiment structure

The goal of this investigation is to evaluate different modelling and prediction approaches to serve as a basis for SIMSON. Specifically, it will examine three DSM approaches (*inflow-*, *stock-*, and *change*-driven, s. Section 3.4) to inform the SIMSON-MFA model, and three stock prediction techniques (here called *'Pauliuk '*, *'Dürrwächter '* and *'LSTM '*, s. Section 3.5).

A visualisation of the experiment structure is given in Fig. 7. Firstly, three DSM modelling approaches will be used to compute the inflows, stocks, outflows and lifetimes of the in-use steel from 1900-2008 for the twelve REMIND world regions [BBB+21] and four product categories ('Transport', 'Construction', 'Machinery' and 'Products').

Subsequently, the 1900-2008 steel stocks will be used to predict the steel stocks from 2009-2022 with the three prediction techniques. Then, the 2008 lifetimes of each of the three modelling approaches will be used to derive the 2009-2022 inflows from the stock predictions via stock-driven dynamic stock modelling. Next, future trade is predicted assuming that trade will develop proportionally to inflow (s. Section 3.3, based on [PSL23]). Finally, the 2009-2022 production predictions can be calculate from inflow into the use phase and trade and then compare it to the actual production data from the same time span ([WSA23]).

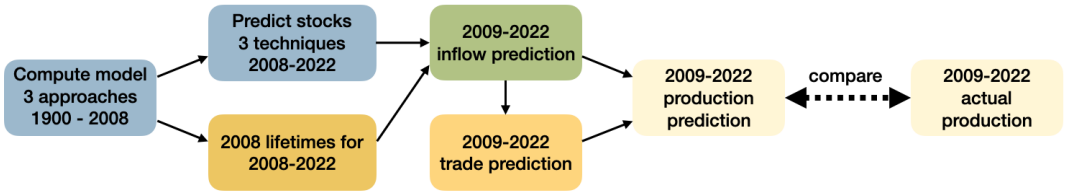

Figure 7: Visualisation of the experiment design.

The year 2008 is chosen as a base year because it was used by Pauliuk et al. [PWMA13] for their predictions and hence can ensure an adequate comparison. Therefore, the 1900-2008 data effectively represents our training data, and the 2009-2022 production as our test data. Overall, the experiment tests with which model approach / prediction technique combination the 2009-2022 period would have been predicted best.

3.2. Data sources & preparation

An overview of the main data sources of the project is given in Table 1. As most of the original datasets were not yet in the desired format, the processing steps taken are described below.

Type	Description & Resolution	Source
Population	Worldwide, 1900-1950	UN [UN99]
Population	All countries, 1950-2100	UN [UN22]
Population	All countries, 5 SSPs, 1965-2100	[KL17]
GDP	Some world regions, 1900-1950	OECD [BTvZ14]
GDP	All countries, 1950-2013	IMF [JGMG12]
GDP	All countries, 5 SSPs, 1965-2100	[KL23]
Steel stocks	All countries, 4 categories, 1900-2008	[PWM13]
Steel stock sector split	All countries, 4 categories	[PWM13]
Steel production	All countries, 1962-2022	WSA [WSA23]
Steel production	Worldwide, 1900-1979	WSA [WSA23]
Steel trade	All countries, 1962-2022	WSA [WSA23]
MFA parameters	Steel lifetime mean & st. dev	[PWMA13]
MFA parameters	Forming Yield	[CAB12]
MFA parameters	Fabrication Yield	[Wit21]

Table 1: Description of data sources, including United Nations (UN), International Monetary Fund (IMF), Organisation for Economic Coordination and Development (OECD) and World Steel Association (WSA) data.

As country-specific population data and predictions were given only for the years 1950-2100 in the primary UN dataset [UN22] and other openly accessible data source for the years 1900-1949 with country specific resolution could not be found (as many country borders changed), the dataset was extrapolated into the past assuming proportional development to world population [UN99].

The same was done for the gross domestic product (GDP) data (given in purchasing power parity (PPP)) with a dataset by the OECD [BTvZ14]. The 1950-1965 period could be extrapolated assuming proportional development to a country specific GDP dataset by the IMF (s. [JGMG12]). The GDP datasets were already adjusted to inflation and are based on the 2005 US-Dollar.

The population data that had scenario specific resolution ([KL17]) was only used for the scenario predictions in Section 5.4. Apart from that section, for the future GDP data, the baseline SSP 2 scenario was assumed.

The population predictions were published in 2017 [KL17] and 2022 [UN22], whilst the GDP predictions were published in 2023[KL23]. For a fair comparison of the prediction techniques, predictions from the year 2008 or before would have been necessary. As such data could not be found, the available data needs to be used. This is taken into account in the discussion (Section 5).

Part of the data, like the steel stock estimates [PWM13] was given per capita, and hence the UN population datasets were used to retrieve the total amounts. Some data given in five- or ten year steps (GDP predictions, 1900-1950 data) was interpolated linearly to get a yearly resolution.

Steel stock information was provided for the four in-use categories transportation,

construction, machinery and products. Estimates for the share of the four product categories in steel stocks [PWM13] were incorporated to estimate sector splits in fabrication (s. Section 3.4.1).

Steel production and steel trade data (both direct and indirect) was taken from the World Steel Association (WSA) [WSA23]. Here direct trade (the trade of crude steel before fabrication) was estimated through the difference of production and apparent use (an estimate of steel demand by the WSA). Similar to population and GDP data, steel production pre-1962 was derived from world production data. Indirect trade (the trade finished steel products) was split into the four in-use categories using 2013 estimates [WSA15].

Extrapolating trade data pre-1962 has the added difficulty that total global imports and exports should be balanced. Pehl et al. addressed this problem when forecasting future trade [PSL23]. Firstly, the trade was kept at the same share in regional use from the last available data point. Subsequently, imports and exports were balanced using Eq. 5 (taken from [PSL23]):

$$T_{r'} = T_r(1 - sign(T_r)\frac{\sum_r T_r}{\sum_r |T_r|}) \tag{5}$$

Here, T_r denotes the regional net trade (imports positive, exports negative), and $T_{r'}$ the balanced regional trade. Hence, imports and exports are scaled inversely by the share of global net trade ($\sum_r T_r$) in global absolute trade($\sum_r |T_r|$). So if for example total global imports exceed exports, imports are scaled down and exports up by the same percentage so that they equal each other.

This technique was adapted here for the past interpolation of trade: the past trade share in production (net trade / production) was kept constant instead of the past trade share in use, as primary data sources were available for production data. However, for the future prediction of trade (s. Fig. 7), the use/inflow was taken again instead, as no future predictions of the production was available (as this is the quantity this thesis aims to estimate).

In SIMSON, the parameters necessary to implement the MFA were taken from a variety of sources and are discussed in more detail in Section 3.3 (also s. Appendix A). The forming yield was estimated to be 93.7246 % based on data from [CAB12]. The fabrication yield for all four categories were based on [Wit21]. The steel lifetime and SD for all four categories were taken from [PWMA13].

When steel data was provided for countries that do not exist anymore, like the former Soviet Union, the amounts where divided into the currently existing countries by the share of GDP in the first year where split data was available. The same logic was applied to GDP data, here share in total population was taken as the dividing factor.

For example, if the steel production in the Soviet Union in 1992 was 100 kT, and the share of the Russian GDP in the summed up GDP of all ex-Soviet Union countries was 80 %, the Russian steel production in that year was estimated to be 80 kT.

3.3. SIMSON upper cycle

While SIMSON and its MFA structure is explained in detail in Appendix A, the only part relevant to this investigation is the 'upper cycle', from production to use-phase. The details of its mechanism necessary for the understanding of the experiments will be outlined in this section. In Fig 8 a simplified version of this part of the steel cycle is portrayed.

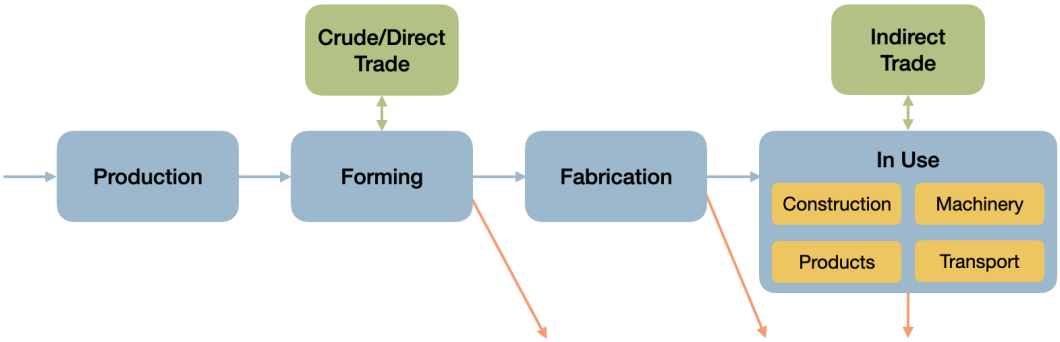

Figure 8: Upper cycle of SIMSON (simplified).

Crude steel is produced in the 'Production' process and then traded (across world regions). Hence the quantity of steel flowing into the forming process is production P and net crude trade T_{Crude} (s. Eq. 6). Here, our data always has two dimensions, time t and region r. Production for the year 2005 in the United States might for example have been one million tonnes of steel.

$$Q_{Available}(t,r) = P(t,r) + T_{Crude}(t,r) \tag{6}$$

In SIMSON, the forming process represents all processes where steel is formed into intermediate products, like hot rolled bars. During such forming, losses occur. The quantity of these losses is defined by the forming yield Y_{Form}, and was estimated to be around 93 % (based on data by Cullen et al. [CAB12]). From here, the quantity of steel flowing into the fabrication process Q_{Form} and the forming losses L_{Form} can be calculated with Eq. 7 and 8.

$$Q_{Form}(t,r) = Q_{Available}(t,r)Y_{Form} \tag{7}$$

$$L_{Form}(t,r) = Q_{Available}(t,r)(1 - Y_{Form}) \tag{8}$$

The quantity of steel coming out of fabrication, so the steel in the newly produced cars, building, etc. is calculated using the fabrication yield, taken from [Wit21]. However, first the sector split $S(t,r,g)$ needs to be estimated, defining how much of the formed steel will be used for each category g. This will be calculated differently for each model approach, see sections 3.4.1-3.4.3.

Each of the four in-use categories g also has a fabrication yield $Y_{Fabr}(g)$ used to calculate how much 'fabricated' steel flows to the use phase ($Q_{Fabr}(t, r, g)$, s. Eq. 9), and how much is lost in fabrication ($L_{Fabr}(t, r, g)$, s. Eq. 10).

$$Q_{Fabr}(t, r, g) = Q_{Form}(t, r)S(t, r, g)Y_{Fabr}(g) \tag{9}$$

$$L_{Fabr}(t, r, g) = Q_{Form}(t, r)S(t, r, g)(1 - Y_{Fabr}(g)) \tag{10}$$

Finally, the inflow into the use phase is defined as the fabrication plus the indirect trade (s. Eq. 11).

$$I(t, r, g) = Q_{Fabr}(t, r, g) + T_{indirect}(t, r, g) \tag{11}$$

The in-use process itself is then realised as a dynamic stock model (or actually several dynamic stock models for each region and in-use good category). It consists of the inflow, stocks, outflow and lifetime data.

3.4. Model approaches

As the different DSM-based modelling approaches were only referenced briefly thus far, this section will go into more detail about their realisation in this investigation.

As described above, production, trade, stock and lifetime data is prepared. With the process described in the previous paragraph (Section 3.3), inflow (also called demand or use) into the use phase can be derived from production and trade data, given that some factor $S(t, r, g)$ to split the fabrication into sectors can be produced. Inflow estimates can also be derived from stocks and lifetimes using *stock-driven* dynamic stock modelling (s. Section 2.1).

Note that the stock data is a secondary data source based on Pauliuk et al.'s work [PWM13] and therefore relies on further assumptions. However, it is still valuable as the MFA that it was derived from has a degree of detail that is beyond the scope of this investigation.

The model approaches tested for the purposes of this thesis are the more commonly used *inflow-driven* and *stock-driven* methods as well as a newly proposed *change-driven* approach. A visualisation of all three is shown in Fig. 9.

In the *inflow-driven* model, inflow data and lifetime assumptions are used to establish a new estimate of steel stocks which is described in Section 3.4.1. The *stock-driven* model uses stocks and lifetimes to estimate inflow and subsequently production (s. Section 3.4.2). Lastly, in the *change-driven* model, Pauliuk et al.'s stock data [PWM13] is used in combination with inflow estimates (from production and trade data) to estimate lifetimes (s. Section 3.4.3). All three models also calculate the outflow to be used further in the MFA cycle calculations (see Appendix A).

As mentioned in Section 3.1, the three modelling approaches are used to estimate the 1900-2008 steel cycle. From there, the 2009-2022 inflow and production is estimated using the *stock-driven* model.

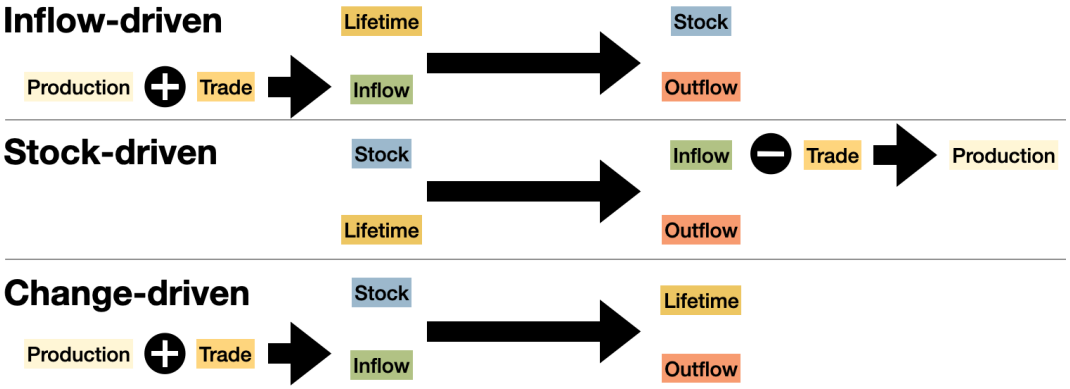

Figure 9: The three model approaches used to set up the MFA. The '+' and '-' here is an abstraction of the process described in Section 3.3.

Whilst both the *stock-driven* and the *change-driven* model use the same stock data initially, their predictions will still be different as they will be based on different lifetime assumptions. Additionally, in the *change-driven* model, the stock data is slightly manipulated, leading to further differences, as outlined in Section 3.4.3.

3.4.1. Inflow-driven model

The *inflow-driven* approach can be implemented mainly using the production to use flow described in Section 3.3. The only unknown value is the sector split $S(t, r, g)$ to split fabrication estimates into the four in-use categories.

Whilst no primary data sources for this fabrication sector split were found, Pauliuk et al. systematically estimated stock sector splits for all countries [PWM13]. Hence, a fabrication sector split that causes the stock change sector split to approach their estimates was calculated:

From the SIMSON 'upper cycle' equations in Section 3.3 we know how to relate the quantity of steel going into the fabrication process $Q_{Form}(t, r)$ to the inflows (Eq. 12).

$$I(t, r, g) = Q_{Form}(t, r)S(t, r, g)Y_{Fabr}(g) + T_{indirect}(t, r, g) \tag{12}$$

Let us simplify this by removing the region (r) dimension, as the same method can be applied across regions. Further, we relabel $Q_{Form}(t, r) = F(t, r)$, $T_{indirect}(t, r, g) = T(t, r, g)$ and $S(t, r, g) = x(t, r, g)$ as this is the variable we are searching for. The result is Eq. 13:

$$I(t, g) = F(t)x(t, g)y(g) + T(t, g) \tag{13}$$

If in every year, the stock change sector split will approach Pauliuk et al.'s estimates ([PWM13]), this will also be true for the total stock change (s. Eq. 2). From dy-

namic stock modelling (Section 2.1), we know how to relate inflows to stock change. Equation 14 shows an expansion of the DSM equations:

$$\begin{aligned} S_c(t,g) &= I(t,g) - O(t,g) \\ &= I(t,g) - \sum_{t' \leq t} I(t',g)\lambda(t,t',\tau,\sigma) \\ &= I(t,g) - I(t,g)\lambda(t,t,\tau(g),\sigma(g)) - \sum_{t'<t} I(t',g)\lambda(t,t',\tau(g),\sigma(g)) \\ &= I(t,g)(1-\lambda(t,t,\tau(g),\sigma(g))) - \sum_{t'<t} I(t',g)\lambda(t,t',\tau(g),\sigma(g)) \end{aligned} \tag{14}$$

Here, the subtrahend $\sum_{t'<t} I(t',g)\lambda(t,t',\tau(g),\sigma(g))$ denotes the outflow of the past cohorts. We will relabel this $O_p(t,g)$. In the first year, this quantity is zero ($O_p(t=0,g)=0,\forall g$).

We also know stock change sector split $c(g)$ and can define it by relating it to the stock change $S_c(t,g)$ (s. Eq. 15).

$$c(g) = \frac{S_c(t,g)}{\sum_g S_c(t,g)}, \forall t \tag{15}$$

Let G be the set of in use good, so that $g \in G$. Let us further assume there are goods $a, b \in G$. We can now combine Eq. 14 and Eq. 15 to relate the sector split and the inflow in Eq. 16 as we do not know the stock change itself yet (as this is the quantity we want to find out in the *inflow-driven* model).

$$\begin{aligned} \frac{S_c(t,a)}{S_c(t,b)} &= \frac{c(a)\sum_g S_c(t,g)}{c(b)\sum_g S_c(t,g)} \\ &= \frac{c(a)}{c(b)} \\ &= \frac{I(t,a)(1-\lambda(t,t,\tau(a),\sigma(a))) - O_p(t,a)}{I(t,b)(1-\lambda(t,t,\tau(b),\sigma(b))) - O_p(t,b)} \end{aligned} \tag{16}$$

Let us further simplify this using variables $l(t,a,b) = c(b)(1-\lambda(t,t,\tau(a),\sigma(a)))$, $s(t,a,b) = c(b)O_p(t,a)$ and $l(t,b,a)$ and $s(t,b,a)$ vice versa. We also expand the inflows using Eq. 13 in Eq. 17.

$$\begin{aligned} I(t,a)l(t,a,b) - s(t,a,b) &= I(t,b)l(t,b,a) - s(t,b,a) \\ \frac{(F(t)x(t,a)y(a) + T(t,a))l(t,a,b) - s(t,a,b)}{(F(t)x(t,b)y(b) + T(t,b))l(t,b,a) - s(t,b,a)} &= 1 \end{aligned} \tag{17}$$

Now we can express $x(t,b)$ in terms of $x(t,a)$ in Eq. 18.

$$x(t,a)\frac{y(a)l(t,a,b)}{y(b)l(t,b,a)} + \frac{T(t,a)l(t,a,b) - T(t,b)l(t,b,a) - s(t,a,b) + s(t,b,a)}{F(t)y(b)l(t,b,a)} = x(t,b) \tag{18}$$

We also know that $\sum_g x(t,g) = 1$. Now if we see Eq. 18 as a linear function with y-intercept $n(t,a,b) = \frac{T(t,a)l(t,a,b) - T(t,b)l(t,b,a) - s(t,a,b) + s(t,b,a)}{F(t)y(b)l(t,b,a)}$ and gradient $m(t,a,b) = \frac{y(a)l(t,a,b)}{y(b)l(t,b,a)}$, we can solve for x in Eq. 19:

$$\begin{aligned} x(t,a)m(t,a,b) + n(t,a,b) &= x(t,b) \\ \sum_{b \in g} x(t,a)m(t,a,b) + n(t,a,b) &= 1 \\ \frac{1 - \sum_{b \in g} n(t,a,b)}{\sum_{b \in g} m(t,a,b)} x(t,a) &= x(t,a) \end{aligned} \tag{19}$$

This can be done for all $a \in g$. As a last consideration, the inflows need to be positive. This might not always happen as the outflows and indirect exports in a specific year and category might be so high that the inflows can not 'make up' for it.

In these cases, we use Eq. 20 to define the minimum of the sector split $x(t,g)$:

$$\begin{aligned} I(t,g) = F(t)x(t,g)y(g) + T(t,g) &\geq 0 \\ x(t,g) &\geq \frac{-T(t,g)}{F(t)y(g)} \\ x(t,g)_{min} &= \frac{-T(t,g)}{F(t)y(g)} \end{aligned} \tag{20}$$

To comply with this minimum, we therefore in those cases adjust x slightly using Eq. 21.

$$x(t,g)_{final} = max(x(t,g)_{min}, x(t,g) - \frac{x(t,g) - x(t,g)_{min}}{\mid \frac{\sum_g max(0, x(t,g) - x_{min}(t,g))}{\sum_g min(0, x(t,g) - x_{min}(t,g))} \mid}) \tag{21}$$

We can calculate the final inflow with Eq. 13 and then obtain the stocks with the lifetime data and inflow-driven dynamic stock modelling. Note that x needs to be calculated iteratively for every time step as $O_p(t,g)$ is based on all inflows of the last years and therefore x will have to have been calculated for all those years.

3.4.2. Stock-driven model

For the implementation of the *stock-driven* model, no adjustments needed to be made. The stock and lifetime data could be used directly to infer inflows via dynamic stock modelling and calculate production from there.

Specifically, we can transform Eq. 14 to solve for inflow as shown in Eq. 22.

$$\begin{aligned} S_c(t,g) &= I(t,g)(1-\lambda(t,t,\tau(g),\sigma(g))) - O_p(t,g) \\ I(t,g) &= \frac{S_c(t,g)+O_p(t,g)}{(1-\lambda(t,t,\tau(g),\sigma(g)))} \end{aligned} \tag{22}$$

We know the stock change from the stock data, λ from the lifetime data, and O_p (the outflow from the past cohorts) is zero in the first year and can be calculated iteratively using the past inflows. This is automatically done using the ODYM library [PH19]. Finally outflows can be calculated subtracting stock change from inflows (s. Eq. 1).

3.4.3. Change-driven model

One of the main concerns with the *stock-driven* model is that even if the lifetime estimates are plausible, there might be a big gap between inflows derived from the model and real-world inflows as this investigation does not use the exact same model Pauliuk et al. used to create the dataset [PWM13]. Additionally, the lifetimes given are used across all years (the t/time dimension), and the lifetime of steel products might have significantly changed over the last decades.

Idea To solve this, the novel method of the *change-driven* model is introduced here: using production and trade data to calculate inflows (like in the *inflow-driven* model, s. Section 3.4.1) and estimate lifetimes on a year by year basis from inflow and stock *change*. Subsequently, outflow can be derived from the difference in inflow and stock change (derived from the stock data). The lifetime calculation is presented in detail below and is necessary for the stock-driven prediction later on.

The main idea of the *change-driven* model is to use Eq. 14 similarly to how it is used in the *stock-driven* model, but to derive lifetimes from inflow and stock change as shown in Eq. 23.

$$\lambda(t,t,\tau(g),\sigma(g)) = 1 - \frac{S_c(t,g)+O_p(t,g)}{I(t,g)} \tag{23}$$

We can then do an iterative calculation of λ starting in the base year (and, like in Section 3.4.2, calculate $O_p(t,g)$ iteratively as well). From there, we can calculate the mean and SD of the lifetimes of the products in each year. Before that, we further assume that the lifetime SD is 30 % of the mean as proposed by Pauliuk et al. [PWMA13], so $\sigma = 0.3\tau$. Eq. 23 can be solved then for the mean, because when $t' = t$, λ (Eq. 3) can be simplified as outlined in Eq. 24.

$$\begin{aligned}\lambda(t,t,\tau,\sigma) &= \frac{1}{\sqrt{2}\pi\sigma}e^{\frac{-(t-t-\tau)^2}{2\sigma^2}} \\ &= \frac{1}{\sqrt{2}\pi 0.3\tau}e^{\frac{-(0-0-\tau)^2}{2(0.3\tau)^2}} \\ &= \frac{1}{\tau\sqrt{2}\pi 0.3e^{\frac{1}{2*0.3^2}}} = \lambda(\tau)\end{aligned} \tag{24}$$

And hence, when $t = t'$, Eq. 25 shows how to compute lifetime mean τ from λ.

$$\tau = \frac{1}{\lambda(\tau)\sqrt{2}\pi 0.3e^{\frac{1}{2*0.3^2}}} \tag{25}$$

There are a couple of technicalities to consider when implementing the change based model. Firstly, according to the stock estimates from Pauliuk et al. [PWM13], there was some stock of steel already prevalent in the base year (1900). Therefore, the stock change in that year is a lot higher than in the next years. As the production data is not as high in the first year, this might create negative outflows, which are unrealistic.

Consequently, in the *change-driven* model inflows are set equal to the stock change only for the first year. As this inflow of steel should also reach an end of life and hence leave the use-phase at some realistic point, this cohort is assumed to have half of the normal lifetime (hence assuming it to an average have 'lived' half its life thus far), using Pauliuk's lifetime assumptions only this once ($\tau(0,g) = \tau_{Pauliuk}(g)/2$, $\sigma(0,g) = \sigma_{Pauliuk}(g)/2$). Subsequently, Eq. 22 can be used to find the inflows in the base year via Eq. 26:

$$I(0,g) = \frac{S_c(o,g)}{1-\lambda(0,0,\tau(0,g),\sigma(0,g))} \tag{26}$$

Production in the base year can be calculated from there using Eqs. 6 - 11.

Sector split for change driven model Apart from the first year where a given lifetime is assumed, the sector split $x(t,g)$ in the *change-driven* model is not given and hence inflows can not be calculated simply from production. The same method as in the *inflow-driven* model (s. Section 3.4.1) can not be used because here lifetime estimates are not used (as this is the quantity being calculated by the *change-driven* model). However, an estimation of the sector split can be made:

As before, the fabrication sector split is going to be derived from the stock change sector split. Revisiting Eq. 22, we notice that the only variable we do not know is λ. However, we also know that λ defines the outflow of the current cohort in the current year. This is the steel products reaching their end of life in the year that they are produced.

This quantity should be quite small and therefore not greatly affect the fabrication sector split. Conclusively, the best approach is to assume it to be zero for the purposes of estimating the fabrication sector split as shown in Eq. 27.

$$\begin{aligned} I(t,g) = F'(t)x(t,g)Y(g) + T(t,g) &= S_c(t,g) + O_p(t,g) \\ F'(t)x(t,g) &= \frac{S_c(t,g) + O_p(t,g) - T(t,g)}{Y(g)} \end{aligned} \tag{27}$$

Note that $F'(t)$ here will not be equal to the $F(t)$ calculated from production data as we ignored λ for the purposes of finding the sector split. As we know that the sum of the sector splits needs to be 1 (100 %, $\sum_g x(t,g) = 1$), we can find $F'(t)$ from the other parameters and then solve for $x(t,g)$ as Eq. 28 shows.

$$\begin{aligned} F'(t) &= \sum_g \frac{S_c(t,g) + O_p(t,g) - T(t,g)}{Y(g)} \\ x(t,g) &= \frac{\frac{S_c(t,g)+O_p(t,g)-T(t,g)}{Y(g)}}{\sum_g \frac{S_c(t,g)+O_p(t,g)-T(t,g)}{Y(g)}} \end{aligned} \tag{28}$$

Plausible Lifetimes As a last consideration, in the way described above, the change-based model is very sensitive to tiny changes in λ and as it is found iteratively, small mistakes in some years might lead to problems in others (e.g. this method does not rule out negative or otherwise implausible lifetimes).

Hence, after finding λ and the lifetimes, the final found lifetime mean τ_{final} is limited to be within a factor of 5 of the lifetime mean proposed by Pauliuk.

$$\tau_{final} = max(\frac{\tau_{Pauliuk}}{5}, min(5\tau_{Pauliuk}, \tau)) \tag{29}$$

In the case where $\tau_{final} \neq \tau$, we then again derive the final lifetime SD using the factor 0.3 ($\sigma_{final} = 0.3\tau_{final}$) and then adapt the final stock change using Eq. 14. This is what causes the different stock data in the *stock-driven* and *change-driven* model.

3.5. Prediction techniques

Using the three described model approaches, three sets of 1900-2008 stock data and 2008 lifetime data can be computed to serve as a basis for the stock predictions. In this section, *Pauliuk*, *Dürrwächter* and *LSTM* predictions that use these outputs will be described in more detail. In Table 2 the main differences between the techniques are summarised.

Whilst a couple of other prediction techniques exist (s. [PSL23, YWM21]), these have been chosen as they portray a variety of methods and shapes. *Pauliuk* and *Dürrwächter* both use the idea of a saturation level (sat-level), but divert in how it is implemented. While the *Dürrwächter* technique is novel, it uses many ideas from Pehl

Name	Method	Shape	Sat-level	Use of GDP data
Pauliuk	Formula	S-shaped	pre-defined	indirect (sat-level)
Dürrwächter	Formula	concave	fitted to data	direct (fitting)
LSTM	Machine Learning	various	no	direct (training)

Table 2: Overview of the investigated prediction techniques.

et al. [PSL23] such as finding the formula parameters through optimisation. *LSTM* has not yet been used in this field but has proven its use in other areas ([SNTSN18], [SK18]).

The adaptation of Pauliuk et al.'s prediction approach [PWMA13] is outlined in Section 3.5.1. In Section 3.5.2 the formula and implementation of the prediction technique based on ideas by Dr. Dürrwächter is presented. Lastly, how the LSTM model was set up and trained is described in Section 3.5.3.

3.5.1. Pauliuk prediction

Pauliuk et al.'s idea is rooted in the assumption that steel stocks saturate with increasing economic development. They calculate steel stocks per capita with a formula similar to the sigmoid function (Eq. 30). However, the independent variable of their formula is not a term expressing economic development (like GDP) but time. They still incorporate assumptions on economic development by pre-defining a saturation level $\hat{S}$ and a saturation time t_s by which that saturation is fulfilled. The authors that using GDP estimates would "merely shift the uncertainty from our own estimate to an exogenous forecast" [PWMA13].

$$S(t) = \frac{\hat{S}}{1 + (\frac{\hat{S}}{S_0} - 1)e^{c(1-e^{d(t-t_0)})}} \tag{30}$$

Here, S_0 is the level of stocks per capita in the base year, t_0 the last year where data is available (here 2008), t the year for which the stock level is supposed to be determined and c and d are constants. These constants are needed to skew the curvature of the predicted stock levels to fulfil two conditions:

1. The stock curve is tangent to the latest historic stock ($t_0 = 2008$).
2. The per capita stocks reach 99% of the saturation level at the saturation time t_s.

To calculate c and d, we can derive new equations from these conditions. For condition 1, we firstly need the derivative of the stock curve, shown in Eq. 31.

$$S'(t) = \frac{\hat{S}cd(\frac{\hat{S}}{S_0} - 1)e^{c(1-e^{d(t-t_0)})+d(t-t_0)}}{((\frac{\hat{S}}{S_0} - 1)e^{c(1-e^{d(t-t_0)})} + 1)^2} \tag{31}$$

Now we can set this equal to the gradient g that we know from the stock per capita data in year $t_0 = 2008$. The gradient here is simply the difference in stock per capita to last years data, but at least 0.001 ($g = max(S(t) - S(t-1), 0.001)$). This is because, dependent on the model approach (s. Section 3.4), the gradient in our stock data could sometimes be negative which does not work with this technique as the gradient of a sigmoid-shaped curve is never negative. As $t = t_0$ and $t_0 - t_0 = 0$ a lot of the derivative equation is simplified as shown by Eq. 32.

$$S'(t_0) = g = \frac{\hat{S}cd(\frac{\hat{S}}{S_0} - 1))}{(\frac{\hat{S}}{S_0})^2} \tag{32}$$

We further simplify this in Eq. 33 by introducing the constant h:

$$\frac{g(\frac{\hat{S}}{S_0})^2}{\hat{S}(\frac{\hat{S}}{S_0} - 1)} = h = cd \tag{33}$$

Note that in Pauliuk et al.'s approach $\frac{\hat{S}}{S_0} - 1 > 0$ holds as the saturation level is assumed to be over the current stock levels and hence, $h > 0, c \neq 0, d \neq 0$. Again, this will not necessarily be true for all model approaches in this investigation, and therefore the saturation level is slightly altered in such cases: $\hat{S} = max(S_0 * 1.02, \hat{S}_{Pauliuk})$.

Next, we can demonstrate the second condition in mathematical terms in Eq. 34:

$$S(t_s) = 0.99\hat{S} = \frac{\hat{S}}{1 + (\frac{\hat{S}}{S_0} - 1)e^{c(1-e^{d(t_s - t_0)})}} \tag{34}$$

This can be transformed to:

$$\frac{\frac{1}{0.99} - 1}{\frac{\hat{S}}{S_0} - 1} = e^{c(1-e^{d(t_s - t_0)})} \tag{35}$$

This can be further simplified in Eq. 32 by introducing two constants, l and v:

$$ln(\frac{\frac{1}{0.99} - 1}{\frac{\hat{S}}{S_0} - 1}) = l = c * (1 - v^d) \tag{36}$$

Here $v = e^{t_s - t_0}$. Hence, $v > 0$. Additionally, we can assume that $S_0 < \hat{S} * 0.99$ due to condition 2. Therefore, $\frac{1}{0.99} < \frac{\hat{S}}{S_0}$ and further $\frac{\frac{1}{0.99} - 1}{\frac{\hat{S}}{S_0} - 1} < 1$. We can conclude that $l < 0$.

It is now established that $l = c * (1 - v^d)$ and $h = cd$. By inserting $c = \frac{h}{d}$, we derive Eqs. 37 and 38:

$$l = \frac{h}{d}(1 - v^d) \tag{37}$$

and (substituting $l/h = m$)

$$v^d + \frac{l}{h}d - 1 = v^d + md - 1 = 0. \tag{38}$$

This formula can be solved for d by taken it as a function $f(d)$, and finding it's first and second derivative (Eqs. 39-41).

$$f(d) = v^d + md - 1 \tag{39}$$

$$f'(d) = v^d ln(v) + m \tag{40}$$

$$f''(d) = v^d ln(v) ln(v) \tag{41}$$

One of the roots of the function will be zero as $f(0) = v^0 + m*0 - 1 = 1 + 0 - 1 = 0$. Given that $d \neq 0$, there has to be another root apart from zero (as Pauliuk et al. chose saturation levels and times so that they found solutions for c and d).

To find its other root, the Newton-Raphson method from SciPy [VGO+20] was used. The Newton-Raphson method is a technique to approximate a root of a function [Che13]. It will converge if the function is convex [Che13]. This is the case here, as all of the factors of $f''(d)$ are positive, and therefore the function is convex. After finding d this way, c can be obtained from d and h using the formula $c = \frac{h}{d}$.

Having found c and d, we can use Eq. 30 to predict future steel stocks per capita. Using the population predictions, future steel stocks can be derived which then can used to predict the rest of the steel cycle as described in Section 3.1.

3.5.2. Dürrwächter prediction

Analysing past stocks and GDP data, Dr. Jakob Dürrwächter suggested that the correlation between per capita stocks and GDP might not follow an s-shaped sigmoid-like formula (as proposed in [PSL23][YWM21]) but rather a normal concave curve (s. Fig. 4). Adapting the assumption that per capita steel stocks will saturate with increasing economic development, he proposed the following formula to relate the two quantities as shown in Eq. 42.

$$S(g) = A(1 - e^{-bg}) \tag{42}$$

Here, S is the steel stocks, g the GDP data (both per capita), and A is the saturation level and b influences the gradient of the curve. Both A and b are unknown.

Whilst the idea and formula for this prediction technique was proposed by Dr. Dürrwächter, the implementation of it is a novel aspect contributed by this investigation.

To find these parameters, the least-squares optimisation method from SciPy was used [VGO+20]. Assuming that the steel stocks of all regions will saturate at a similar level, the optimisations was first done for the whole dateset across world regions to find a global saturation level A.

This found global saturation level A_{global} was highly sensitive to the different combinations of model type, regional resolution (REMIND [BBB+21] vs. 'Pauliuk' ([PWMA13] based on [Lut96]) regions), steel stocks and GDP data source. It ranges from 0.57 to 4652 tonnes/capita. Out of these combinations, 17.4 tonnes/capita was chosen as the resulting value that was most similar to Pauliuk et al.'s estimates [PWMA13].

After a global estimate of the two parameters was found using the least-squares optimisation, then b was regionally adapted using Eq. 43 so that the resulting curve will match the base year (2008) stock level (S_0) at the base year GDP level (g_0).

$$b(r) = -\frac{\ln\left(1 - \frac{S_0(r)}{A_{global}}\right)}{g_0(r)} \tag{43}$$

After obtaining all necessary parameters, the future steel stocks per capita can be predicted by using the GDP predictions and plotting them on the proposed *Dürrwächter* curve. The resulting prediction of steel stocks for the twelve REMIND regions is shown in Fig. 10. Lastly, per capita predictions are transformed to total predictions using the population predictions.

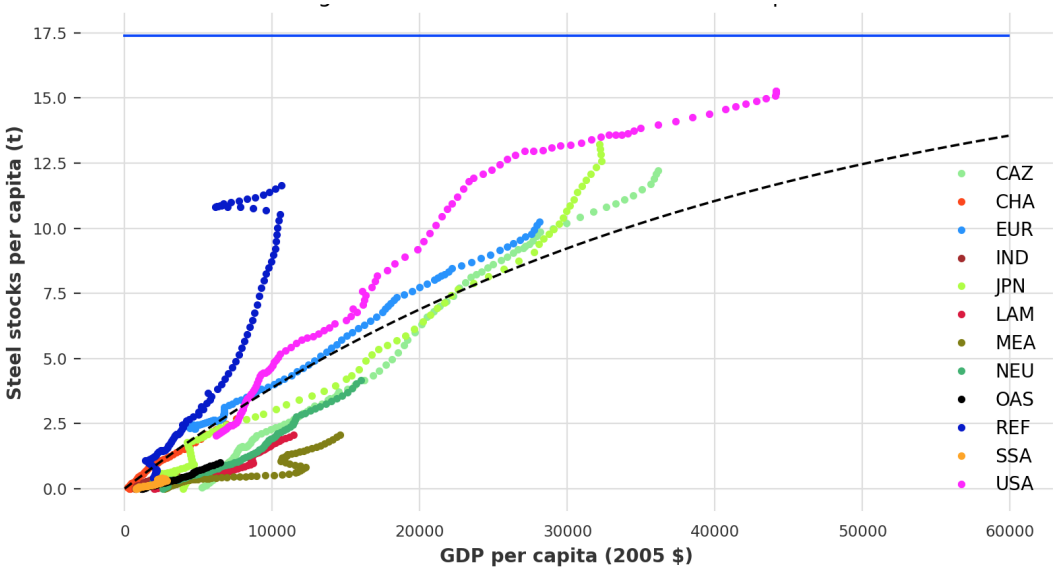

Figure 10: Per capita stocks over GDP per capita and fitted *Dürrwächter* curve for all regions (dashed line) with a saturation level of 17.4 tonnes/capita.

3.5.3. LSTM prediction

There is a multitude of machine learning method types for time series forecasting (TSF) e.g. classical ones (like ARIMA, Exponential Smoothing), Random Forests, and Neural Network based ones like Convolutional Neural Networks and LSTM

Networks [Ger23] and then a variety of options of how to implement a specific method.

Whilst implementing and comparing all options would give the only holistic analysis of to the effectiveness of ML-based solutions in steel cycle prediction, this would be beyond the scope of this investigation.

LSTM-networks were chosen for this project as they have been shown to perform well in comparison with other approaches [SNTSN18] and have been successfully used in similar fields [SK18, KS20]. This section describes how specifically the LSTM-network was implemented.

In simple forecasting methods, a series of past data points is analysed and then the future is predicted from that analysis. However, this approach would not use all available information: it can be assumed that the progression of per capita stocks in one region might develop similarly in another region.

Additionally, as described in Section 2.3, there is a high correlation between per capita steel stocks and GDP. Hence, it would be useful if the resulting model could utilise past and future GDP data to inform its predictions.

The DARTS [HLP+22] Python library was chosen to implement the LSTM-network for this thesis as it fulfils these requirements. The model can be trained iterating through the region data, and GDP (per capita) data can be incorporated using so-called 'future-covariates'. These covariates are passed into the respective LSTM cells as part of the input x (s. Fig. 5).

After choosing the DARTS framework, the last aspect that needs to be defined are the hyperparameters. Optimising all of them again would be beyond the scope of this investigation. Hence, two major parameters, *n-rnn-layers* (the number of RNN layers) and *n-epochs* (the number of epochs trained), were focused on.

Both drastically affect the resulting prediction accuracy but also the degree of overfitting to the past data. For example, technically, the greater the number of epochs, the better the prediction accuracy. However in this case it was observed that sometimes with increasing epochs the models predicted negative stocks due to overfitting.

Therefore, an experiment was conducted pre-evaluating LSTM models with different combinations of values for *n-rnn-layers* (3, 6, 9, 12) and *n-epochs* (300, 600, 900, 1200) for all three model approaches (s. Section 3.4). The results are discussed in Section 4.1.

The output chunk length (number of time steps predicted at once) was chosen to be 14 as ultimately, the years 2009-2022 are supposed to be predicted. Hence, the input chunk length (number of past time steps used at prediction point) used was 95 years, so that the 1900-1994 data could be used to predict the next 14 years until our base year 2008 when evaluating the model (for the pre-evaluation during training the 2009-2022 testing data was not used to have a fair comparison to the other prediction techniques).

For the other parameters liken hidden dimension and batch size, the default DARTS parameters were adopted. An overview of the hyperparameters is given in Table 3.

Parameter	Value	Default
Input chunk length	95	x
Output chunk length	14	x
Number of RNN layers	3-12	x
Number of epochs	300-1200	x
Hidden dimension size	25	✓
Dropout rate	0	✓
Batch size	32	✓

Table 3: Overview of main used hyperparameters for the LSTM network in DARTS [HLP+22].

Lastly, data from the reforming countries (former Soviet Union, 'REF' in Fig. 10) was ignored as an outlier for the *inflow-driven* approach as the irregular decline of the regions steel production greatly affected stock numbers.

3.6. Evaluation

After stocks are predicted, the 2009-2022 production can be derived as described in Section 3.1. Hence, the production predictions of all combinations of the three modelling approaches and the three prediction techniques can be compared.

To evaluate which combination provided the *best* prediction, there are a variety of available metrics. Whilst all measure slightly different aspects, it has been assessed through quantitative research that the differences in the results are often only subtle [DKA22]. This investigation focused on the mean absolute percentage error (MAPE) as it offers an intuitive interpretation, is a popular tool [KK16] and has been used in comparable research [SLWF10].

The formula to calculate the MAPE is shown in Eq. 44 (taken from [KK16]). Here, F_t are the predicted values (forecast) whereas A_t are the values actually observed. The MAPE is undefined if the actually observed values are zero, which in this case is never the case as steel is produced in all world regions.

$$MAPE = \frac{1}{n}\sum_{t}^{n}|\frac{A_t - F_t}{A_t}| \tag{44}$$

Apart from MAPE, the runtime of each combination was measured as well as the model might be coupled with other models in REMIND and hence be able to react quickly.

4. Results

Having described the experiment setup in detail, the results are presented below. Before comparing the performance of the model approach and prediction technique

combinations, the results of the pre-evaluation of the LSTM Models are presented in Section 4.1. Following this, the final results of the combinations and the 2009-2022 production predictions are shown in Section 4.2. Lastly, the runtime of the combinations is compared in Section 4.3.

4.1. Pre-Evaluation of LSTM Models

The results of the test for LSTM performance for different numbers of epochs and RNN-layers are shown in Table 4. They were conducted using the 1900-1994 period as test data and the 1995-2008 period as training data.

inflow	**300**	**600**	**900**	**1200**
3	1.09	0.97	0.7	1.19
6	1.19	2.9	1.03	1.14
9	4.76	3.83	2.75	***0.49***
12	18.63	2.4	1.73	2.9
stock	**300**	**600**	**900**	**1200**
3	1.02	1.7	0.94	1.57
6	2.61	1.51	0.71	***0.58***
9	4.26	22.96	3.49	1.41
12	2.34	1.34	0.93	6.67
change	**300**	**600**	**900**	**1200**
3	3.34	***0.55***	2.46	0.78
6	0.97	1.33	0.6	2.48
9	4.47	1.55	1.25	4.83
12	2.52	0.71	3.52	1.98

Table 4: Evaluation LSTM-network with different combinations of numbers of RNN-layers (rows) and epochs (columns). Results are given for all three modelling approaches using MAPE (in %).

In general, the results got slightly better with increasing number of epochs, but less RNN-layers yielded better results. However, the correlation is small in both cases. For all three model approaches, a network with a MAPE of less than 1 % for the test data set could be found.

The best performing network was chosen and is emphasised in Table 4. In none of these cases the network predicts negative stocks.

4.2. Predictions

The results of the predictions of worldwide steel production of the combinations of model approaches and prediction techniques are shown in Fig. 11 and compared to real world data (orange line).

Overall, especially the *change-driven* model in combination with *LSTM* and *Dürrwächter* prediction seem to predict worldwide production reasonably well (MAPE below 5 %).

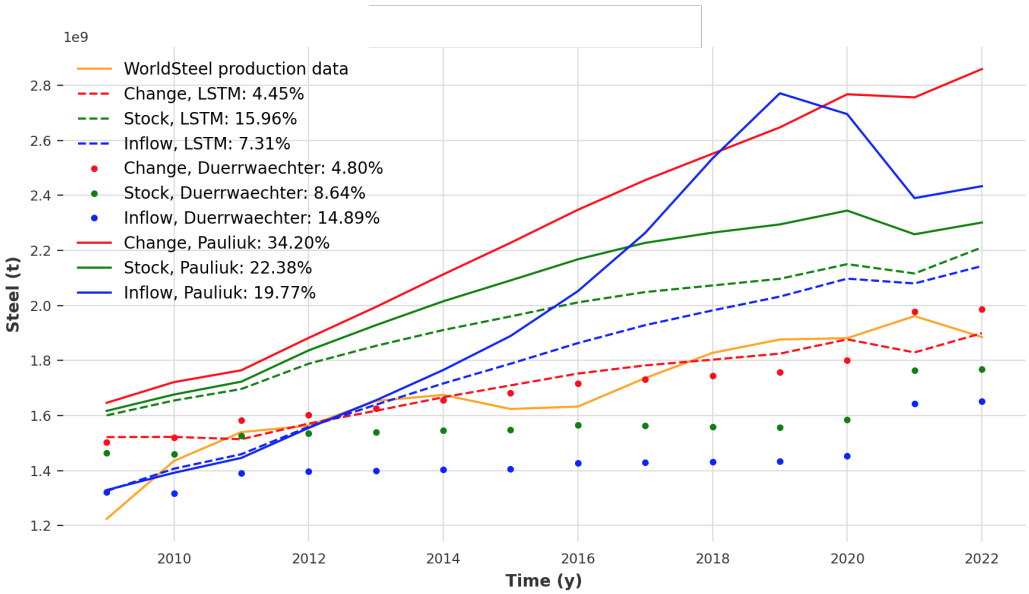

Figure 11: Final results of production predictions for all combinations with MAPE given in %. The orange line shows the actually observed production data from the World Steel Association [WSA23] as a comparison.

A summary of the MAPE of the different combinations is given in Table 5. Here, an evaluation is made both for total global production and as an average across regional errors. Noticeably, the regional predictions have a lot higher error rates than the summed global production predictions with on average a roughly four times higher MAPE.

For the global error results, the *change-driven* model combined with the *LSTM* prediction performs best, whereas for regional predictions, the *inflow-driven* model combined with the *Dürrwächter* prediction yields the best results.

On average, the *inflow-driven* model and the *LSTM* prediction perform best in both global and regional error assessments.

4.3. Runtime

To determine the runtime of the model approach/prediction technique combinations, each combination was run 100 times and an average was calculated. The tests were conducted on a 2.7 GHz Dual Core processor with 8 GB RAM. The results are given in Table 6.

Overall, the *change-driven* models ran quicker than the others, and the combina-

Global	*Pauliuk*	*Dürrwächter*	*LSTM*	*average*
Inflow	19.77	14.89	7.31	**13.99**
Stock	22.38	8.64	15.96	15.66
Change	34.2	4.8	**4.45**	14.48
average	25.45	9.44	**9.24**	14.71

Region	*Pauliuk*	*Dürrwächter*	*LSTM*	*average*
Inflow	55.65	**40.21**	48.71	**48.19**
Stock	59.27	56.67	45.12	53.69
Change	85.95	69.46	63.13	72.85
average	66.96	55.45	**52.32**	58.24

Table 5: Final evaluation combinations of model approaches (rows) and prediction techniques (columns) using MAPE (in %). Results are given both for the error in total global production and as an average across regional production forecasts. Averages are presented for model approaches and prediction techniques

Runtime	*Pauliuk*	*Dürrwächter*	*LSTM*	*average*
inflow	13.06	12.25	12.48	12.69
stock	11.96	12.05	12.16	12.06
change	11.81	**11.63**	12.48	**11.97**
average	12.28	**11.98**	12.47	12.24

Table 6: Runtime (in seconds) to produce complete model of all model approach & prediction technique combinations, with averages.

tions using *Dürrwächter* predictions outperformed the others, both with an average below twelve seconds. However in both cases the performance was less than 3% better than the overall average.

For both the *Dürrwächter* and the *LSTM* prediction techniques the fitting/training of the model was excluded from the runtime tests.

5. Discussion

After presenting the results of the experiments, the performance of the different models is discussed in detail in this section. Additionally some details of the resulting predictions are portrayed.

Whilst accurate regional forecasts would increase the reliability of the model, models that do this better but are worse in estimating global trends will result in worse greenhouse gas emission predictions that matter globally, not regionally (and in turn might affect production). Therefore, the focus is on the result of the global predictions, but the regional forecasts are discussed as well.

In Section 5.1 the performance of the three model approaches is compared and contrasted. The same follows in Section 5.2 for the three prediction techniques. Lastly, the prediction results of the best performing model are analysed in Section 5.3 alongside predictions for the SSP scenarios in Section 5.4.

5.1. Model approaches

In terms of model approaches, the *change-driven* approach appears to predict higher production than the *stock-driven* approach, with the *inflow-driven* approach predicting even less. This is not true for combinations using *LSTM* predictions. This is caused by higher stock estimates in the inflow-driven approach (and smaller ones in the change driven one), leading to smaller increases in stock levels for the prediction techniques using saturation levels (*Pauliuk* and *Dürrwächter*).

The *inflow-driven* approach performed best on average. However, the resulting stock predictions are, as expected, very sensitive to changes in production. For example, the massive decline of the Soviet steel production due to its dissolution at the beginning of the 1990's resulted in a sudden decline of stocks in the model.

This should be addressed when using the model in the future by for example treating such occurrences as outliers as described in Section 3.5.3. Nevertheless the estimates of the stocks seem altogether quite plausible and are roughly in the same range as the data from Pauliuk et al. [PWM13](s. Fig. 14).

Whilst the best performing model in terms of predicting global production used the *change-driven* approach (s. Table 5), the lifetime calculation of the model failed to produce realistic estimates, s. Fig 12.

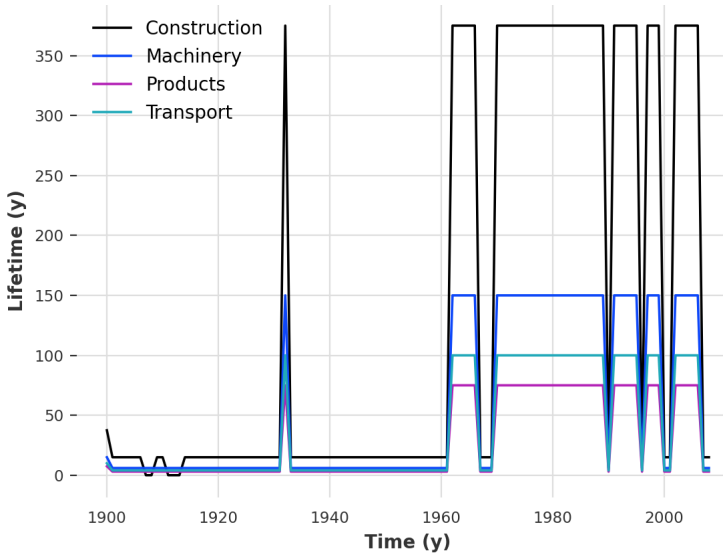

Figure 12: The resulting lifetime estimates for Latin America ('LAM') for the four in-use categories in the *change-driven* model.

The values switch repeatedly between the given maximum and minimum values. For example, the Latin American lifetime estimates for construction switch a lot between the minimum value $75/5 = 15$ years and the maximum value $75 * 5 = 375$ (s. Section *change-driven* for calculation of minimum and maximum lifetime). This was expected for some years where production or stock data suddenly changed, but a constantly occurring tremendous change of lifetime is unrealistic.

This is probably due to the lifetime calculation being so dependent on the outflow of products in the year that they are produced (s. Section 3.4.3). These are usually minimal and hence small errors here cause large problems overall.

The main issue is that the resulting lifetimes for the year 2008 are used to predict future production based on stock-driven dynamic stock modelling. Whilst this might not greatly affect short term predictions like the ones conducted here, constantly too low or too high lifetimes as a basis of predictions will be implausible in the long run.

5.2. Prediction techniques

Overall, the *Pauliuk* and the *LSTM* prediction tend to over-predict production (especially the former) whereas the *Dürrwächter* prediction appears to under-predict. Whilst for the saturation based approaches *Pauliuk* and *Dürrwächter* this could be simply solved by increasing/decreasing the saturation level (or changing the saturation time), this showcases the difficulty of estimating these parameters.

Here it needs to be pointed out that whilst the estimates of saturation levels and times by Pauliuk et al. where published in 2013, the other two prediction techniques could use up-to-date population and GDP data as input for their stock predictions of the years 2009-2022. Additionally, the authors might have adapted their estimations to the REMIND regions differently than done here (s. Section B).

However, for the training/fitting of the models, the *Dürrwächter* and *LSTM* prediction techniques had the same data available. Due to the significantly better average global performance of these two compare to the *Pauliuk* prediction (about 16 % better MAPE), the results suggest that they are more accurate at least in their production predictions, which was the goal for this investigation.

Notably, the *LSTM* prediction yielded the best results (s. Table 5) even though the network was only optimised in terms of number of RNN-layers and epochs. However, predictions were highly sensitive to the random initialisation of weights and biases in the network. This is not surprising given that the training dataset consisted of only 12 x 95 x 2 = 2280 data points (number of regions and years for both stock and GDP data).

Therefore theoretically LSTM-networks with a better performance on the training dataset might be found that predict negative or otherwise implausible (like highly fluctuating) stock values. For example, the resulting prediction second best *LSTM* prediction for the *change-driven* model approach in the LSTM pre-evaluation (with a MAPE of 0.6 instead of 0.55 %, s. Table 4) is shown in Fig. 13. In the non-EU ('NEU')

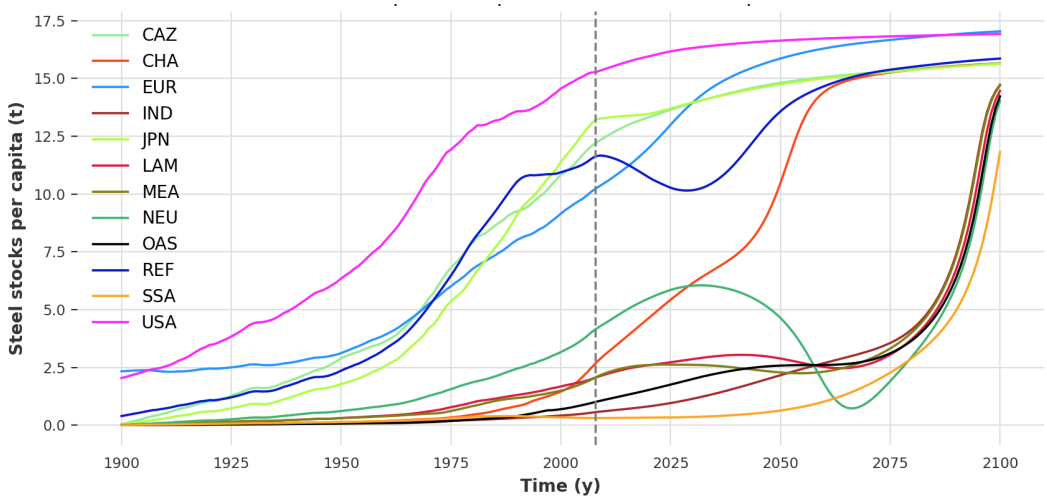

Figure 13: Per capita stock prediction of the second best model combination: *change-driven / LSTM* .

region, there is a sudden drop in the per capita stock prediction around 1940 which seems highly unrealistic.

This could potentially be addressed with some form of supervised learning where experts discourage certain undesired outputs like suddenly changing stock levels.

5.3. Analysis of predictions

Lastly, the steel cycle predictions for the best models according to this investigation can be assessed. Due to the problems in the *change-driven* model approach described in Section 5.1, the model approach/prediction technique combination with the best global MAPE that does not use the *change-driven* model was chosen. This is the *inflow-driven / LSTM* combination with a global MAPE of 7.31 %.

The resulting per capita stock prediction for the twelve REMIND regions [BBB+21] is shown in Figure 14. Interestingly, an S-shaped sigmoid-like form similar to the *Pauliuk* predictions can also be observed with the *LSTM* forecasts (s. Section 3.5.1, [PWMA13]). However, not a complete saturation seems to occur, indicating that also in developed regions per capita stocks will continue to increase.

Additionally, Pauliuk et al. assume the saturation times for developing countries in e.g. Asia and Africa to be around 2150 [PWMA13] whereas they appear to occur a lot earlier here. This might be due to the GDP predictions used here opposed to the information used by Pauliuk et al. to determine their saturation times.

This however shows how significant good economic forecasts are as they massively affect the production and ultimately greenhouse gas emission forecasts as will be shown in the following paragraphs.

The resulting projected production is shown in Figure 15. It predicts a peak of

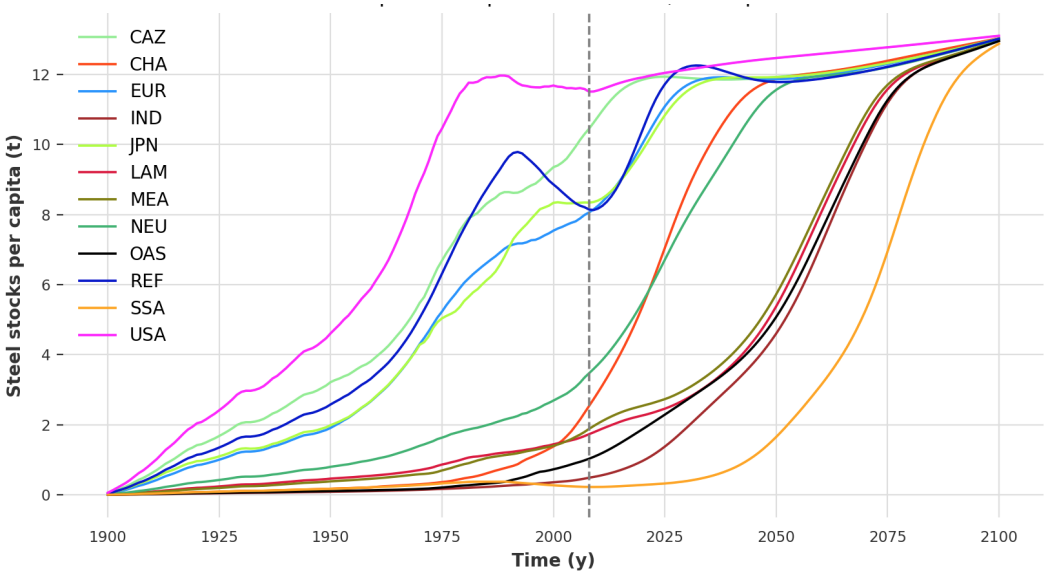

Figure 14: Per capita stock prediction of the *inflow-driven / LSTM* model.

Chinese (CHA) steel production around 2030 (which is in accordance with the Chinese' governments pledge to reach the peak of carbon emissions by 2030 [CXGL22]).

India (IND), Other Asia (OAS), Latin America (LAM) and the Middle East (MEA) are projected to have their peak in steel production around 2065 whilst Sub-Saharan Africa (SSA) is set to have a massive increase in production peaking around 2080.

When comparing the total global production predictions of the *inflow-driven / LSTM* model with the approach taken by Pauliuk et al. in their predictions [PWMA13] (here adapted as *stock-driven / Pauliuk*) it becomes apparent that in fact, the former predictions are a lot higher in the second half of the century whilst being roughly comparable in the first, s. Fig. 16.

Specifically, the cumulative production predictions of the *inflow-driven / LSTM* model are 10 % higher than the *stock-driven / Pauliuk* model by 2066 and 25 % higher by the end of the century.

Lastly, the results of the regional forecasts were a lot worse than the total global forcasts, with a roughly seven times higher MAPE for the *inflow-driven / LSTM* model. As an example, Fig. 17 depicts the predictions for Latin America. This could be partly due to faulty trade predictions (s. Section 3.2), especially as the net global production is so much better.

However, it might also be cause by the structure of the prediction process: predicting per-capita stocks first and ultimately deriving inflow and production from there. This might work well to establish long term trends, but fail to capture short term changes in production.

Hence, it might be fruitful to combine predictions solely based on production trends with this long-term stock-based prediction approach.

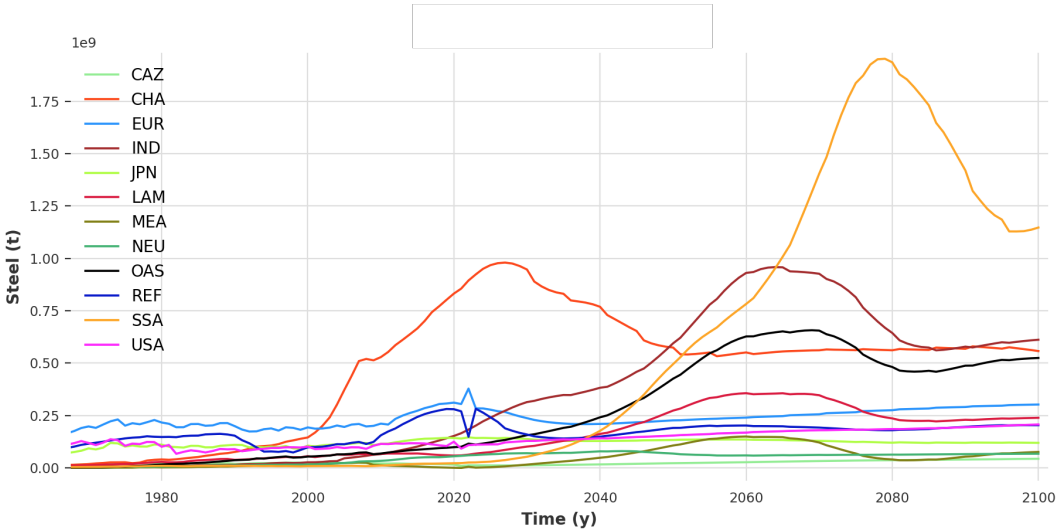

Figure 15: Production prediction of the *inflow-driven / LSTM* model.

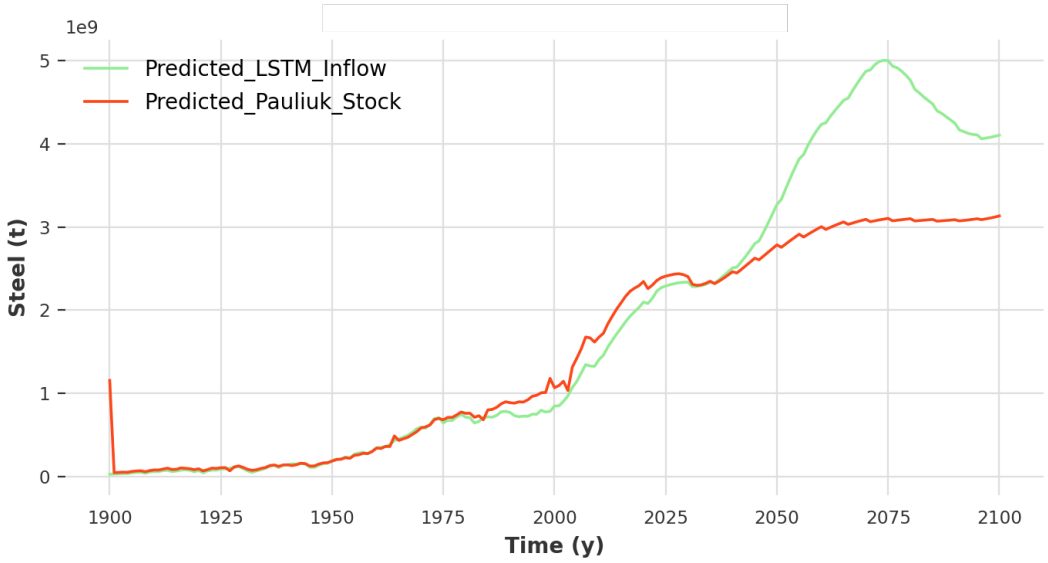

Figure 16: Total global production prediction of the *inflow-driven / LSTM* model vs the *stock-driven / Pauliuk* model.

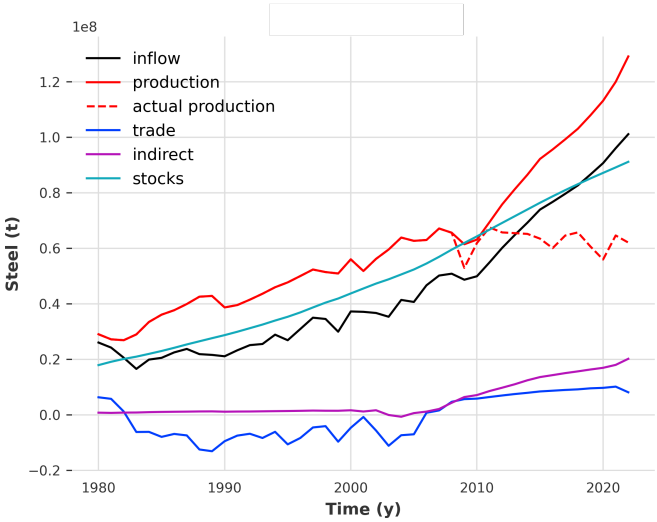

Figure 17: Steel cycle predictions of flows and stocks for Latin America (LAM) in the *inflow-driven / LSTM* model. Production predictions are compared to actually recorded production.

5.4. SSP scenario predictions

The GDP per capita and population projections for the five SSP scenarios can be used as an input to the *LSTM* network to subsequently obtain production predictions for the scenarios. In Fig. 18, such predictions of the *inflow-driven / LSTM* combination model are compared with the GDP per capita predictions for the scenarios.

Due to the observed correlation of GDP and stocks per capita, it was expected that scenarios with high GDP per capita projections like SSP1 and SSP5 would also have the highest steel production. However, this was not observed with the *LSTM* -based models.

Potentially, this might be caused by the predicted GDP per capita of SSP3 and SSP4 following a concave and not convex trajectory which has not been observed in the training data. However, this highlights a weakness of the machine learning based approach as different from the *Pauliuk* and *Dürrwächter* prediction, the network cannot explain its reasoning.

Hence, for comparison of different trajectories of SSP scenarios, it may be better to take a model that does not use *LSTM* prediction. In Fig. 19, the production forecasts for the scenarios for the *inflow-driven / Dürrwächter* model is shown.

Here, the hypothesis of high GDP projections causing high production forecasts is fulfilled due to the nature of the *Dürrwächter* prediction technique.

However, according to O'Neil et al. (2014), SSP1 is supposed to be the most sustainable scenario. This needs to be taken into account when using these prediction

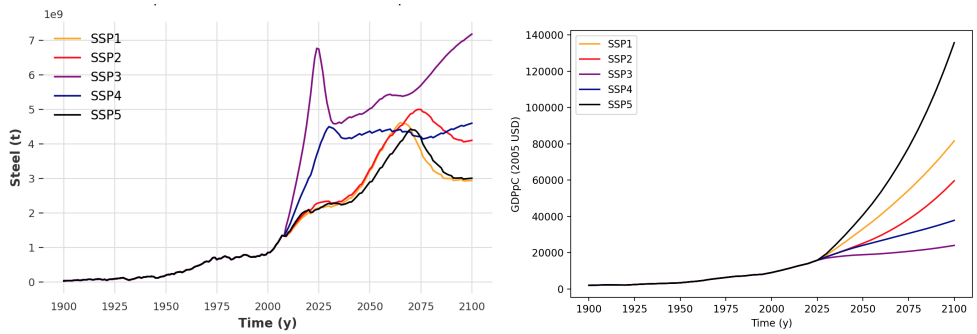

Figure 18: Steel production projection for the five SSP scenarios in the *inflow-driven / LSTM* model (left) vs. GDP per capita development (right).

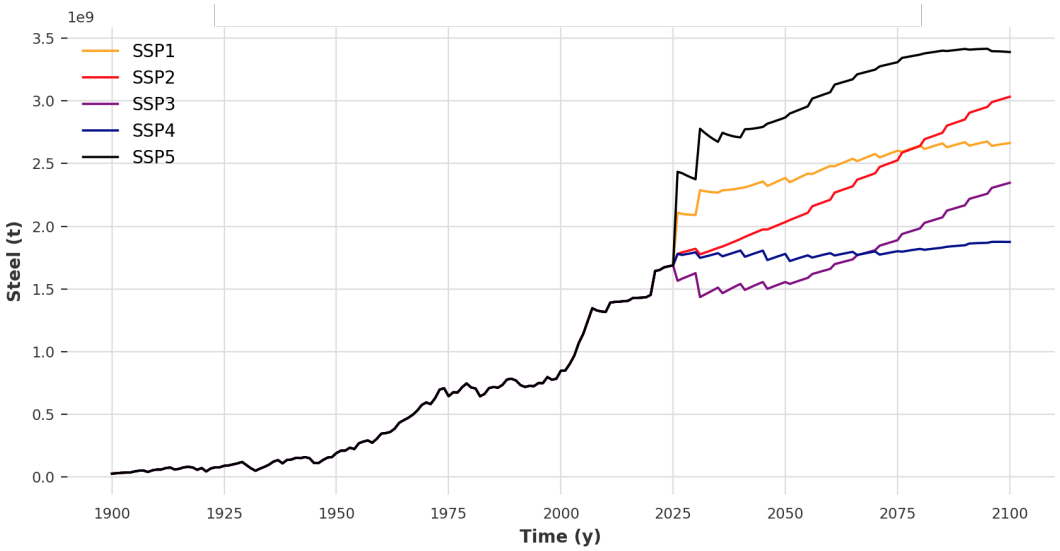

Figure 19: Steel production projection for the five SSP scenarios in the *inflow-driven / Dürrwächter* model.

models, e.g. by introducing higher recycling rates for SSP1 in SIMSON or manually adapting production according to SSP (as for example suggested in [PSL23]).

6. Conclusion

In this investigation, three steel cycle modelling approaches (*inflow-driven*, *stock-driven* and *change-driven*) and three steel stock prediction techniques (*Pauliuk*, *Dürrwächter* and *LSTM*) were compared in their accuracy to predict global steel production.

Data available in 2008 was used to predict the next fifteen years, making the time span 1900-2008 the training period and 2009-2022 the testing period of the models.

Overall, the *inflow-driven* model approach and the machine learning based *LSTM* prediction performed best. However, the limitations of the ML approach of being very sensitive to hyperparameters and initialisation were discussed.

Whilst the *change-driven* approach resulted in well-performing predictions for the 2009-2022 period, the found lifetimes are implausible. As an alternative to the *LSTM* prediction, the *Dürrwächter* technique performed second-best and was also the technique with the fastest runtime.

Taking this into account, there are various possibilities to improve the described methods. As an outlook on possible future work, a couple of considerations are discussed below.

Firstly, the *change-driven* approach produced the two best performing models but produced implausible lifetimes. It might be worth exploring other ways of deriving lifetime estimates from stocks and inflows that do not depend so much on the outflow of products in the year that they are produced.

One option might be to assume constant lifetimes over past years for all product categories. The optimum lifetime could be found assuming it to be zero at first and slowly increasing it until production data derived from *stock-driven* dynamic stock modelling roughly equals actual production data.

Using the 2009-2022 production data and some lifetime estimates, stock data up to 2022 could be expanded using *inflow-driven* dynamic stock modelling. This data could subsequently be used to make new predictions based on current data.

Here, all prediction techniques could be amended using the updated stock data, the *Dürrwächter* technique by fitting, the *LSTM* net by training the net and the *Pauliuk* approach by potentially changing the saturation levels and times.

For now, most of the predictions are based on projections of GDP. Other data, like potential steel price development might further improve these predictions. This is already currently being investigated via an economic-model extension for SIMSON. Additionally, steel (or steel scrap prices) could be implemented as another *covariate* in the LSTM net.

Further, geographical parameters like population density might help inform predictions - scarcely populated areas might need more per capita steel stocks for bridges and tunnels.

In addition, all described prediction approaches derive production predictions from stock predictions. The concept behind this, to compute demand from the services steel products provide (s. [PFH+21]), seems sensible in the long term. However, as discussed in Section 5.2, it might be fruitful to combine long-term stock predictions with short-term production predictions.

This investigation only implemented a basic LSTM network. Future research could expand upon this work by further optimising the parameters, working on overfitting and the network architecture in general.

Additionally, other ML-based prediction approaches like Random Forests could be tested in their ability to predict steel cycle processes. This could be especially effective as the strength of LSTMs is their ability to 'remember' long-term dependencies which is potentially undesirable in some cases. A comparison of different ML-based techniques via an experiment setup similar to this thesis might be informative here.

References

[BBB+21] Lavinia Baumstark, Nico Bauer, Falk Benke, Christoph Bertram, Stephen Bi, Chen Gong, Jan Dietrich, Alois Dirnaichner, Anastasis Giannousakis, Jérôme Hilaire, David Klein, Johannes Koch, Marian Leimbach, Antoine Levesque, Silvia Madeddu, Aman Malik, Anne Merfort, Leon Merfort, Adrian Odenweller, and Gunnar Luderer. Remind2.1: transformation and innovation dynamics of the energy-economic system within climate and sustainability limits. *Geoscientific Model Development*, 14:6571–6603, 10 2021.

[BNA+22] I.A. Bashmakov, L.J. Nilsson, A. Acquaye, C. Bataille, J.M. Cullen, S. de la Rue du Can, M. Fischedick, Y. Geng, and K. Tanaka. Industry. in ipcc, 2022: Climate change 2022: Mitigation of climate change. contribution of working group iii to the sixth assessment report of the intergovernmental panel on climate change. Technical report, IPCC, 2022.

[BSK19] Pritika Bahad, Preeti Saxena, and Raj Kamal. Fake news detection using bi-directional lstm-recurrent neural network. *Procedia Computer Science*, 165:74–82, 2019. 2nd International Conference on Recent Trends in Advanced Computing ICRTAC -DISRUP - TIV INNOVATION , 2019 November 11-12, 2019.

[BTvZ14] Jutta Bolt, Marcel Timmer, and Jan Luiten van Zanden. Gdp per capita since 1820. In *How was Life?: Global Well-being since 1820*, chapter 3, pages 57–72. OECD publiching, 2014.

[CAB12] Jonathan Cullen, Julian Allwood, and Margarita Bambach. Mapping the global flow of steel: From steelmaking to end-use goods. *Environmental science technology*, 46, 11 2012.

[Che13] Steve Cheng. Newton's method works for convex real functions, 3 2013. Accessed: 20124-02-20 via planetmath.org.

[CXGL22] Jiandong Chen, Chong Xu, Ming Gao, and Ding Li. Carbon peak and its mitigation implications for china in the post-pandemic era. *Scientific Reports*, 12:3473, 03 2022.

[DKA22] Fotios Petropoulos Diamantis Koutsandreas, Evangelos Spiliotis and Vassilios Assimakopoulos. On the selection of forecasting accuracy measures. *Journal of the Operational Research Society*, 73(5):937–954, 2022.

[Ger23] Oleksandr Gerasymov. Using machine learning for time series forecasting project, Jan 2023.

[HLP+22] Julien Herzen, Francesco Lässig, Samuele Giuliano Piazzetta, Thomas Neuer, Léo Tafti, Guillaume Raille, Tomas Van Pottelbergh, Marek Pasieka, Andrzej Skrodzki, Nicolas Huguenin, Maxime Dumonal, Jan Koscisz, Dennis Bader, Frédérick Gusset, Mounir Benheddi, Camila Williamson, Michal Kosinski, Matej Petrik, and Gael Grosch. Darts: User-friendly modern machine learning for time series. *Journal of Machine Learning Research*, 23(124):1–6, 2022.

[HS97] Sepp Hochreiter and Jürgen Schmidhuber. Long short-term memory. *Neural computation*, 9:1735–80, 12 1997.

[IEA22] IEA. Iron and steel technology roadmap. Technical report, International Energy Agency, 2022.

[JGMG12] Spencer James, Paul Gubbins, Christopher Murray, and Emmanuela Gakidou. Developing a comprehensive time series of gdp per capita for 210 countries from 1950 to 2015. *Population health metrics*, 10:12, 07 2012.

[KK16] Sungil Kim and Heeyoung Kim. A new metric of absolute percentage error for intermittent demand forecasts. *International Journal of Forecasting*, 32(3):669–679, 2016.

[KL17] Samir KC and Wolfgang Lutz. The human core of the shared socioeconomic pathways: Population scenarios by age, sex and level of education for all countries to 2100. *Global Environmental Change*, 42:181–192, 2017.

[KL23] Johannes Koch and Marian Leimbach. Ssp economic growth projections: Major changes of key drivers in integrated assessment modelling. *Ecological Economics*, 206:107751, 2023.

[KS20] Zahra Karevan and Johan A.K. Suykens. Transductive lstm for time-series prediction: An application to weather forecasting. *Neural Networks*, 125:1–9, 2020.

[Lut96] Wolfgang Lutz. *The future population of the world: what can we assume today*. London : Earthscan Publ., IIASA, 1996.

[MLL+13] Daniel Müller, Gang Liu, Amund Løvik, Roja Modaresi, Stefan Pauliuk, Franciska Steinhoff, and Helge Brattebø. Carbon emissions of infrastructure development. *Environmental Science and Technology*, 47:11739–11746, 09 2013.

[Mun21] Jaimin Mungalpara. What is lstm , peephole lstm and gru? Nerd For Tech, Apr 2021.

[OKR+14] Brian O'Neill, Elmar Kriegler, Keywan Riahi, Kristie Ebi, Stéphane Hallegatte, Timothy Carter, Ritu Mathur, and Detlef Vuuren. A new scenario framework for climate change research: The concept of shared socioeconomic pathways. *Climatic Change*, 122, 02 2014.

[Pau11] Stefan Pauliuk. A more general mfa system without quantification, 2011. Wikimedia Commons, `File:MFASystem_2.png`.

[PFH+21] Stefan Pauliuk, Tomer Fishman, Niko Heeren, Peter Berrill, Qingshi Tu, Paul Wolfram, and Edgar G. Hertwich. Linking service provision to material cycles: A new framework for studying the resource efficiency–climate change (recc) nexus. *Journal of Industrial Ecology*, 25(2):260–273, 2021.

[PH19] Stefan Pauliuk and Niko Heeren. Odym—an open software framework for studying dynamic material systems: Principles, implementation, and data structures. *Journal of Industrial Ecology*, 24, 10 2019.

[PSL23] Michaja Pehl, Felix Schreyer, and Gunnar Luderer. Modelling long-term industry energy demand and co 2 emissions in the system context using remind (version 3.1.0), unpublished. 08 2023.

[PWM13] Stefan Pauliuk, Tao Wang, and Daniel Müller. Steel all over the world: Estimating in-use stocks of iron for 200 countries. *Resources Conservation and Recycling*, 71:22–30, 02 2013.

[PWMA13] Stefan Pauliuk, Rachel Waugh, Daniel Müller, and Julian Allwood. The steel scrap age. *Environmental Science and Technology*, 03 2013.

[Rit20] Hannah Ritchie. Sector by sector: where do global greenhouse gas emissions come from? *Our World in Data*, 2020. https://ourworldindata.org/ghg-emissions-by-sector.

[RTLW+22] Leon Rostek, Meta Thurid Lotz, Sabine Wittig, Andrea Herbst, Antonia Loibl, and Luis Tercero Espinoza. A dynamic material flow model for the European steel cycle. Working Papers "Sustainability and Innovation" S07/2022, Fraunhofer Institute for Systems and Innovation Research (ISI), 2022.

[SK18] Alaa Sagheer and Mostafa Kotb. Time series forecasting of petroleum production using deep lstm recurrent networks. *Neurocomputing*, 323, 10 2018.

[SLWF10] Haiyan Song, Gang Li, Stephen Witt, and Baogang Fei. Tourism demand modelling and forecasting: How should demand be measured? *Tourism Economics*, 16, 03 2010.

[SNTSN18] Sima Siami-Namini, Neda Tavakoli, and Akbar Siami Namin. A comparison of arima and lstm in forecasting time series. In *2018 17th IEEE International Conference on Machine Learning and Applications (ICMLA)*, pages 1394–1401, 2018.

[UN99] UN. The world at 6 billion. 1 1999. Reference: ESA/P/WP.154 data retrieved from UN, accessed 07.07.23, https://www.un.org/development/desa/pd/content/world-six-billion.

[UN22] UN. Steel statistical yearbook 1978-2019, 2022. data retrieved from UN, accessed 13.07.23, https://population.un.org/wpp.

[VGO+20] Pauli Virtanen, Ralf Gommers, Travis E. Oliphant, Matt Haberland, Tyler Reddy, David Cournapeau, Evgeni Burovski, Pearu Peterson, Warren Weckesser, Jonathan Bright, Stéfan J. van der Walt, Matthew Brett, Joshua Wilson, K. Jarrod Millman, Nikolay Mayorov, Andrew R. J. Nelson, Eric Jones, Robert Kern, Eric Larson, C J Carey, İlhan Polat, Yu Feng, Eric W. Moore, Jake VanderPlas, Denis Laxalde, Josef Perktold, Robert Cimrman, Ian Henriksen, E. A. Quintero, Charles R. Harris, Anne M. Archibald, Antônio H. Ribeiro, Fabian Pedregosa, Paul van Mulbregt, and SciPy 1.0 Contributors. SciPy 1.0: Fundamental Algorithms for Scientific Computing in Python. *Nature Methods*, 17:261–272, 2020.

[Wit21] Sabine Wittig. Quantifizierung und modellierung des stahlrecyclings in europa, 2021.

[WSA15] WSA. Indirect trade in steel. Technical report, 3 2015.

[WSA23] WSA. Steel statistical yearbook 1978-2022. Technical report, World Steel Association, 2023. data retrieved from WSA, accessed 05.06.23, https://worldsteel.org/steel-by-topic/statistics/steel-statistical-yearbook/.

[YWM21] Ryosuke Yokoi, Takuma Watari, and Masaharu Motoshita. Future greenhouse gas emissions from metal production: Gaps and opportunities towards climate goals. *Energy Environmental Science*, 15, 01 2021.

A. Specifics of SIMSON

After introducing the steel cycle model SIMSON (Simulating In-use Material Stocks with the ODYM Network) in Section 2.5 and describing parts of its functionality in Section 3.3, a more detailed description of the model is given here.

An overview of the calculation of the flows is presented in Appendix A.1. A more detailed description of the calculation of the two steel production routes is given in Appendix A.2. Lastly, the aspects of the model that are not used in this thesis but part of the code (Appendix A.4) are outlined in Appendix A.3.

A.1. Flows

Variables are black, constants are grey.

$I(g)$ and $O(g)$ are the inflows and outflows as calculated in the dynamic stock modelling. T refers to net trade data (crude, indirect, scrap) and could be specified to imports (T^I) and exports (T^E). Y are production yields (forming, fabrication), D distributions (taken from [Wit21]), V other values/parameters. P refers to the total production of crude steel, S to the total amount of scrap.

For all flows, losses are not considered yet. F_{A-B} denotes the flow between process A and B as labelled in Fig. 6. All process outside of the system boundary are considered to be part of the 'Environment'/Env process (all trade and the iron production).

$$F_{Env-Use} = T^I_{indirect}(g) \tag{45}$$

$$F_{Use-Env} = T^E_{indirect}(g) \tag{46}$$

$$F_{Fbr-Use}(g) = I(g) - T^I_{indirect}(g) + T^E_{indirect}(g) \tag{47}$$

$$F_{Fbr-Scr}(g) = F_{Fbr-Use}(g)(\frac{1}{Y_{Fbr}(g)} - 1) \tag{48}$$

$$F_{Frm-Fbr} = \sum_g (F_{Fbr-Use}(g) + F_{Fbr-Scr}(g)) \tag{49}$$

$$F_{Frm-Scr} = \frac{F_{Frm-Fbr}}{Y_{Frm}} - F_{Frm-Fbr} \tag{50}$$

$$F_{Env-Frm} = T^I_{crude} \tag{51}$$

$$F_{Frm-Env} = T^E_{crude} \tag{52}$$

$$P = F_{Frm-Fbr} + F_{Frm-Scr} + T^E_{crude} - T^I_{crude} \tag{53}$$

$$F_{Use-Scr}(g,w) = (O(g) - T^E_{indirect}(g))D_{Use-Scr}(g,w) \tag{54}$$

$$F_{Env-Scr}(w) = T^I_{scrap}(w) \tag{55}$$

$$F_{Scr-Env}(w) = T^E_{scrap}(w) \tag{56}$$

$$S_{available}(w) = \sum_{g} F_{Use-Scr}(g, w) + T_{scrap}(w) + F_{Fbr-Scr} + F_{Frm-Scr} \tag{57}$$

$$S_{recyclable} = \sum_{w} S_{available}(w) D_{Scr-Rcy} \tag{58}$$

$$S_{prod-usable} = min(S_{recyclable}, PV_{maxScrapShareProduction}) \tag{59}$$

$$F_{EAF-Frm} = min(0, \frac{\frac{S_{prod-usable}}{P} - V_{scrapShareBOF}}{1 - V_{scrapShareBOF}})P \tag{60}$$

$$F_{Rcy-EAF} = F_{EAF-Frm} \tag{61}$$

$$F_{BOF-Frm} = P - F_{EAF-Frm} \tag{62}$$

$$F_{Rcy-BOF} = F_{BOF-Frm} V_{scrapShareBOF} \tag{63}$$

$$F_{Env-BOF} = F_{BOF-Frm} - F_{Rcy-BOF} \tag{64}$$

$$F_{Scr-Rcy} = F_{Rcy-EAF} + F_{Rcy-BOF} \tag{65}$$

$$F_{Scr-Wst} = \sum_{w} S_{available} - F_{Scr-Rcy} \tag{66}$$

A.2. Calculation of EAF/BOF Route

Once we know how much steel is produced in a country (P), and how much scrap goes into that production (S), we need to know how much of the scrap goes into the basic oxygen furnace (BOF) production route, and how much into the electric arc furnace (EAF) production route. For this, we use two assumptions:

1. We assume the scrap share in the BOF to be the constant rate $b = S_{BOF}/P_{BOF}$, which is usually around 22 %.

2. We assume that 100 % of the steel in the EAF route is from steel scrap.

Now let us build some equations to get x, which we define as the share of steel produced in the EAF route out of the total production.

$$x = \frac{P_{EAF}}{P} \tag{67}$$

$$b = S_{BOF}/P_{BOF} \tag{68}$$

$$S_{EAF} = P_{EAF} \tag{69}$$

$$P_{BOF} + P_{EAF} = P \tag{70}$$

$$S_{BOF} + S_{EAF} = S \tag{71}$$

$$P_{BOF} + Px = P \tag{72}$$

$$P_{BOF} = P - Px \tag{73}$$

$$bP_{BOF} + S_{EAF} = S \tag{74}$$

$$bP_{BOF} + P_{EAF} = S \tag{75}$$

$$bP_{BOF} + Px = S \tag{76}$$

$$b(P - Px) + Px = S \tag{77}$$

$$P(b(1 - x) + x) = S \tag{78}$$

$$\frac{S}{P} - b = -bx + x = x(1 - b) \tag{79}$$

$$\frac{\frac{S}{P} - b}{1 - b} = x = \frac{P_{EAF}}{P} \tag{80}$$

This is all assuming that $S > S_{BOF} = bP_{BOF}$, so that the available scrap can supply enough scrap to make a scrap in BOF rate of around 22% 'happen'. If this is not the case, $x = \frac{P_{EAF}}{P}$ is assumed to be zero (as it should not be negative) and all of the remaining scrap is used in the BOF.

This is all a very rough estimation of the BOF/EAF flows and only based on the scrap in BOF rate. Further research can use BOF/EAF data directly or find out the shares of the routes for each region.

A.3. Other functionalities

The functionalities of SIMSON that are not used in the thesis but are part of the code are the *simulation module*, the *economic module* and further *SSP modelling options*.

The *simulation module* allows users of the model to iteratively run the model with various choices of parameters to compare how these parameter choices affect the predictions. For example, this would allow comparing the accumulation of scrap for different estimations of the forming yield. The simulation module uses an intuitive Microsoft Excel sheet as an interface so that researchers that do not know Python can access the model easily.

The *economic module* uses price elasticities to determine steel demand. Hence, when inputting potential trajectories of the steel and scrap price, the flows of SIMSON are adapted so that e.g. when the steel price decreases, demand increases. The economic module was designed by Dr. Dürrwächter and implemented by Merlin Hosak.

Lastly, the *SSP modelling options* denote a set of functionalities to manually adapt flows according to SSP. For example, the recycling rates for the various steel scrap categories might be adapted. It could be assumed that in the more sustainable SSP1 scenario, the steel recycling rates increase by 5 % until the end of the century. Other parameters that can be adapted using these modelling options are the inflow/demand, the steel reuse rate and the steel price trajectory for the economic model.

A.4. Code

The code for SIMSON including the experiments used in this investigation can be accessed on GitHub via this link: `https://github.com/Merjo/bsc_2024_merlin`. All code was written by Merlin Jo Hosak, except the 'customize' and 'generate_yml' functions in the file
'src/tools/config.py', a total of 29 lines written by Dr. Dürrwächter and ammended by Merlin Hosak that are marked accordingly.

B. Mapping of regions

For the implementation of the *Pauliuk* prediction (s. Section 3.5.1), saturation levels and saturation times for the ten regions used by Pauliuk et al. ([PWMA13], based on [Lut96]) were mapped to the twelve REMIND regions [BBB$^+$21].

The region mapping applied is shown in Table 7. Some 'Pauliuk' regions got mapped to two REMIND regions (like Western Europe to EU and non-EU), meaning that both of those regions were allocated the saturation times and levels of the 'Pauliuk' region 'Western Europe' (WEU).

'Pauliuk' region	**REMIND Region**
Latin America (LAM)	Latin America (LAM)
Developing Asia (DVA)	Other Asia (OAS)
Africa (AFR)	Sub-Saharan Africa (SSA)
Western Europe (WEU)	European Union (EUR), Non EU (NEU)
Middlea East (MES)	Middle East and Africa (MEA)
Commonwealth of Independent States (CIS)	Reforming economies (REF)
Developed Asia and Oceania (DAO)	Japan (JPN)
China (CHA)	China (CHA)
India (IND)	India (IND)
North America (NAM)	Canada, Australia and New Zealand (CAZ), USA (USA)

Table 7: Mapping of regions used by Pauliuk et al. [PWMA13] (based on [Lut96]) to REMIND regions [BBB$^+$21].